2011-01-01

Development Of A Low-Cost Network Of Webcams For Monitoring Plant Phenology In A Chihuahuan Desert Shrubland

Libia Gonzalez
University of Texas at El Paso, lgonzalez16@miners.utep.edu

DEVELOPMENT OF A LOW-COST NETWORK OF WEBCAMS FOR MONITORING PLANT PHENOLOGY IN A CHIHUAHUAN DESERT SHRUBLAND

LIBIA GONZALEZ-ALONSO, B.Sc.

Environmental Science Program

APPROVED:

Craig E. Tweedie, Ph.D.

Thomas E. Gill, Ph.D.

Vanessa Lougheed, Ph.D.

Carl Lieb, Ph.D.

Benjamin C. Flores, Ph.D.
Dean of the Graduate School

DEVELOPMENT OF A LOW-COST NETWORK OF WEBCAMS FOR MONITORING PLANT PHENOLOGY IN A CHIHUAHUAN DESERT SHRUBLAND

by

LIBIA GONZALEZ-ALONSO, B.Sc.

THESIS

Presented to the Faculty of the Graduate School of

The University of Texas at El Paso

in Partial Fulfillment

of the Requirements

for the Degree of

MASTER OF SCIENCE

Environmental Science Program

THE UNIVERSITY OF TEXAS AT EL PASO

December 2011

Acknowledgements

I want to thank my advisors Dr. Craig E. Tweedie, Dr. Thomas E. Gill, Dr. Vanessa Lougheed and Dr. Carl Lieb, for their faith in me, from the initial to the final level, helping me with the development an understanding of my project. It is hard to extend my gratitude for all the people who made this thesis possible. Furthermore, I want to thank all the students and staff from the Systems Ecology Lab (Ari Kassin, Mayra Melendez, Christian Andresen, Christine Laney, and Paul Hotchkin) for their enthusiasm, their inspiration, for providing encouragement, great ideas, and making my journey a fun experience. I am grateful to my Jornada Teammates (Jose Herrera, Gesuri Ramirez, and Aline Jaimes) for their good company in tough times, and for their support. I owe my deepest gratitude to Geovany Ramirez creator of the "Phenology Analyzer", which was essential software for my thesis. It is an honor for me to form part of the Cyber-ShARE Center of The University of Texas at El Paso and I would like to show my gratitude for supporting my project. I am grateful to Jornada Experimental Range LTER program and Down Browning for providing valuable help for the realization of this project. I also would like to thank my parents (Samuel Gonzalez, and Libia Alonso) and brother (Samuel Gonzalez) for their unconditional support, their guidance, wise advice, and for helping me get through all my challenges. To them I dedicate this thesis. Finally, for all those who supported me in the completion of this project I offer my regards and blessings.

This material is supported by the National Science Foundation (NSF) under CREST Grant No. HRD-0734825. All the ideas, outcomes, and conclusions given in this work are those of the author(s) and do not necessarily reflect the views of NSF.

NOTE: This thesis was submitted to my Supervising Committee on November 25, 2011.

Abstract

Phenology is the study of the timing of natural events such as the schedule of plant life-cycle events like bud burst, flowering, seed set and senescence. Many factors control plant phenological dynamics including climate. As such, phenology has been shown in published literature to be one of the best biological indicators of climate variability and change. Recent advantages in digital photography and digital image processing have opened new opportunities for inexpensive, repeatable and automated capture of plant and landscape phenological dynamics. This technology, however, remains poorly studied in terms of its capacity to depict the development of different plant phenophases, and correlate with indices typically used on satellite platforms for remotely sensing land surface properties such as above ground green plant biomass. The overarching goal of this thesis is to develop and test a network of phenocams on the Jornada Experimental Range in a northern Chihuahuan Desert shrubland ecosystem. This study links: (1) field based phenophase monitoring (2) output from a network of webcams, and (3) spectral indices from a Robotic tram system that measures hyperspectral reflectance.

Phenophase development of five dominant plant species differed between species and between years for the same species. The timing of bud break and the presence of green leaves for dominant shrub species closely matched trends in landscape phenology derived from a network of four Microsoft Vx7000 webcams, which were found to be the most cost effective and spectrally sound camera of four different models tested. Greenness indices derived for determination of landscape phenological trends were calculated with new software co-developed with graduate students in the Department of Computer Science and UTEP's Cyber-ShARE Center of Excellence. Greenness indices derived from the webcams correlated well with the normalized difference vegetation index (NDVI) derived for two shrub species (*Prosopis glandulosa*, honey mesquite; and *Larrea*

tridentata, creosote bush) from a robotic tram system that was used to measure hyperspectral reflectance with a Unispec dual channel spectrometer on a weekly basis for 110 sampling points along a 110 meter elevated tramline. Correlations were poor for bare ground and two species of graminoids). Although observations were not sustained over multiple years, thereby preventing isolation of specific climatic conditions controlling phenology in this ecosystem, the delay in 2011 phenophase development documented for all species is likely to be a result of drier and warmer conditions experienced during the 2011 growing season and an extreme freeze event which occurred at the study site in early 2011.

This study has established a baseline set of phenological measurements and tested and developed a relatively unique assemblage of research infrastructure that will be sustained beyond the study period of this thesis. Based on findings that species responded differently in their phenophase development, and the same species demonstrated a hypothesized response to climate variability; it is likely that sustained phenological observations will facilitate isolation of climatic factors controlling phenophase development and dynamics of landscape phenology. These findings may have strong implications to forecasting the future state of northern Chihuahuan Desert ecosystems, and ecosystem properties and processes such as biodiversity and carbon balance.

Table of Contents

List of Tables

List of Figures

1. Introduction

1.1. DEFINITION AND IMPORTANCE OF PHENOLOGY

Phenology is the study of the timing of natural events such as the schedule of plants' life-cycle events such as bud burst, flowering, seed set and senescence. Phenological observations have been documented for centuries (Bradley et al., 1999; Richardson et al., 2007), but due to increased awareness and sense of urgency relating to how climate change may impact ecosystems phenological observations have been receiving increased attention. This is largely because time series phenological observations offer insight as to how climate variability and climate change may impact the timing of plant cycles. Phenology is well recognized for being an excellent indicator of how biota is affected by climatic and meteorological phenomena (Justice, 1985).

Since the eighteenth century, relating plant phenological patterns to climate has been a subject of scientific study (Aitken, 1974; Bowers and Dimmitt, 1994). Phenological monitoring is a primary focus in the agricultural sciences, where the timing of fruit and flower production can be vital in determining agricultural output (Loomis and Connor 1992; Bowers and Dimmitt, 1994). In managed agricultural settings, the timing of phenophases such as flowering and fruiting affects crucial aspects of plant life cycles such as the timing of flowering and therefore need for pollination, and seed set, which can control harvesting and transport requirements. Monitoring of plant phenology has been found to be reliable for quantifying landscape and ecosystem responses to climate change (Morisette et al., 2009). Phenology most often captures the exact date of key phenological events in interannual cycles, such as summer green up and autumn senescence. Examples in plants include initial growth or emergence of first buds and leaves, when the first flowers and fruits appear, and the date of leaf fall in deciduous species.

Canopy state is a primary control of the spatial and temporal patterns of land-atmosphere exchange of carbon, water and energy (Kurc and Benton, 2010). Recently, repeat observations of canopy phenology using digital cameras have shown to be useful indicators of global change (Schwartz & Reiter, 2000; Cayan et al., 2001; Badeck et al., 2004; Peñuelas 2004; Crimmins and Crimmins, 2008). Digital cameras have also shown to be an efficient way to monitor green-up and senescence in both natural and agricultural ecosystems (Paruelo et al., 2000; Przeszlowska et al., 2006; Vanamburg et al., 2006; Richardson et al., 2007; Ahrends et al., 2008; Campillo et al., 2008; Crimmins and Crimmins, 2008; Kurc and Benton, 2010). Such advances in technology facilitate and automate quantitative description of canopy state and offer enormous potential for improving understanding of both seasonal patterns and responses to variation of canopy phenology in response to climate. For example, some plants respond to changes in climate, through altered timing of phenological states such as emergence from dormancy (Haggerty and Mazer, 2008).

Other studies have shown that plant phenology is not only sensitive to climate itself but also other seasonal events controlled by climate, such as the timing of the first and last frosts, or when ice melts (Haggerty and Mazer, 2008). Several authors mention that the early disappearance of snow reduces flowering dramatically for some species and/or reduces the number of flowers per individual thereby reducing capacities for genetic exchange at the population level (Saavedra et al. 2003; Forrest et al., 2010). Other studies have shown, however, that under extended periods of warming, the flowering period of individual plants can be extended (Dunne et al., 2003). Multiple levels of biological organization can be studied phenologically. Each one of these levels provides essential information about the patterns, processes, and connectivity of biota to other environmental factors, and as such is a fundamental metric for sustained observations of natural and managed ecosystems.

1.2. CONTROL OF PHENOLOGY BY PHYSICAL FACTORS

Phenological activity is influenced by several physical factors that are not always related to climate including light availability, which can vary depending on canopy structure (Huete et al. 2006) soil moisture, and photoperiod length and quality, which can depend on atmospheric conditions (Rathcke and Lacey, 1985; Loomis and Connor, 1992; Kurc and Benton, 2010). Additionally, the geographic distribution of some plant species is fluctuating, and the combined stresses of multiple climatic and other physical factors can also influence phenology (Parmesan and Yohe, 2003; Root et al., 2003; Rosenzweig et al., 2007; Forrest et al., 2010).

1.3. CONTROL OF PHENOLOGY BY BIOLOGICAL FACTORS

Ecosystems and life-forms are strongly influenced by plant phenology, and include interactions among organisms, such as the timing of food availability for pollinators and migratory species. Plants naturally compete with each other for resources such as light, nutrients, water and space - especially if one or more of these are in limited supply. Phenology has a very important role in some competitive situations, and the timing of phenological development is crucial for the survival of some species (Harris, 1977). Researchers have tried to explain the seasonal timing of flowers, in plants that are pollinated by animals for more than a century (Ratchke, 1983; Ratchke and Lacey, 1985; Kochmer and Handel, 1986). Robertson (1985) suggested that the flowering period in plants shifted by natural selection to avoid competition for pollinators. Through evolutionary responses like this, plants have developed several physiological, anatomical, morphological and phenological adaptations that ensure species fitness within ecosystems.

1.4. APPROACHES TO MEASURING PHENOLOGY

Methods for documenting phenological trends include: (1) Traditional plant phenology monitoring, which relies on human observation of phenophases (Richardson et. al., 2009). These

observations are usually made in small areas and with a limited number of individuals. (2) Land surface phenology is measured at larger spatial scales and typically utilizes satellite remote sensing, and spectral indices to quantify seasonal patterns such as bud burst, green-up and senescence of vegetation at landscape to regional scales (White and Nemani, 2006), and (3) And "near-surface" remote sensing, which utilizes spectroradiometric and imaging sensors recording at high temporal resolution to cover plot to landscape levels of spatial integration (depending on the instrument). Recent studies have demonstrated that "near-surface" remote sensing instruments such as imaging sensors ("webcams") present novel capacities for monitoring, assessing and predicting future states of environmental change, in an inexpensive way, even when operated at high frequencies. (Richardson et al., 2007, 2009; Crimmins and Crimmins, 2008; Kurc and Benton, 2010).

1.5. CHALLENGES PHENOLOGICAL SCIENCES

The study of phenological change often requires an observer taking precise measurements of the area of interest. This process must be done efficiently in order to have high quality data, i.e., the observation task is a tedious yet important aspect of this field of research. Moreover, repeating this over time presents a difficult challenge because the observer must be cognizant of small scale change and abide by strict protocols. Although recent technological advancements can aid the capture of a greater range of individuals over a large area, these devices still require periodic calibration and maintenance, and cross correlation with human measurements. Beyond field based observation, other challenges include extrapolation of measurements spatially and temporally, which must include propagation of uncertainty.

1.6. GOALS AND OBJECTIVES

The overarching goal of this thesis is to develop and test a new method for documenting plant phenological change in a northern Chihuahuan Desert shrubland using webcams. To achieve this, this study links: (1) field based phenophase monitoring, (2) acquisition and post-processing of webcam repeat digital photography; and (3) spectral measurements from a robotic tram system that measures hyperspectral reflectance every meter along a 110 meter transect. Specifically, the objectives, and underlying questions of this study are:

(1) Monitor phenophase development of key plant species and their physical environment to determine the following:

   a. Do temporal patterns of phenological development differ between key plant species?

   b. Is plant phenophase development influenced by climate?

(2) Develop a network of webcams and image processing software to automate the acquisition and post-processing of imagery suitable for documenting landscape-level phenological change by answering the following:

   a. What type of camera is best suited to detecting phenological development through the extraction of Red, Green and Blue (RGB) color bands?

   b. Can software be developed to automate the process of digital image acquisition, storage, and analysis?

(3) Compare measurement of landscape-level phenological development using webcams with field-based phenophase measurements and productivity indices of plant productivity derived from hyperspectral reflectance measurements collected with a robotic tram system. This activity specifically addresses the following questions:

a. Do the optical properties captured by webcams correlate with plant phenological dynamics?
b. Do the optical properties captured by webcams capture the spatial and temporal variability of plant productivity indices derived from hyperspectral reflectance measurements?

2. Study area

This study was conducted on the Jornada Experimental Range (JER), which hosts the Jornada Long Term Ecological Research (LTER) Program managed by the US Department of Agriculture (USDA) Agricultural Research Service (ARS) (Fig. 2.1). The JER is located 37 km north of Las Cruces, in southern New Mexico, USA in the northern Chihuahuan Desert, the largest desert in North America (Havstad et al., 2006). The study site (Latitude: 32.581956, Longitude: -106.635025) is located west of the San Andres Mountains, at an elevation of 1188 m, and a moderate slope of ~ 2 degrees (Fig. 2.2) . Dominant plant species include the shrubs Creosotebush (*Larrea tridentata*) and Mesquite (*Prosopis grandulosa*). The site is situated on a piedmont slope with alluvial fan and fan-piedmont soils. The study site includes a range of scientific infrastructure established and maintained by the Systems Ecology Laboratory at the University of Texas at El Paso (www.sel.utep.edu). This infrastructure is designed to measure land-atmosphere exchange of carbon, water and energy, and the associated drivers and controls of these fluxes. Implicit within the design of the infrastructure is the capacity to build algorithms capable of scaling fluxes with remotely sensed measurements. Infrastructure includes an extended open path eddy covariance system, a robotic tram system suitable for measuring hyperspectral reflectance and making other optical measurements, a sensor network with micrometeorological sensors, four phenology webcams, and phenology stations where phenophase development of key plant species is monitored on a regular basis. These infrastructures are described in more detail below in Section 3.

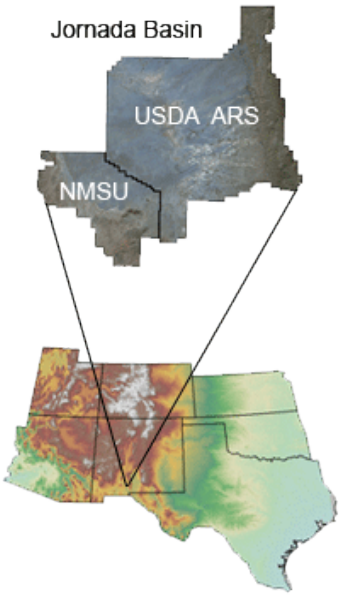

Figure 2.1: The USDA-ARS Jornada Experimental Range (JER) in southern New Mexico. A field station managed by New Mexico State University is located immediately adjacent to the JER. Map courtesy of (www.nmsu.edu).

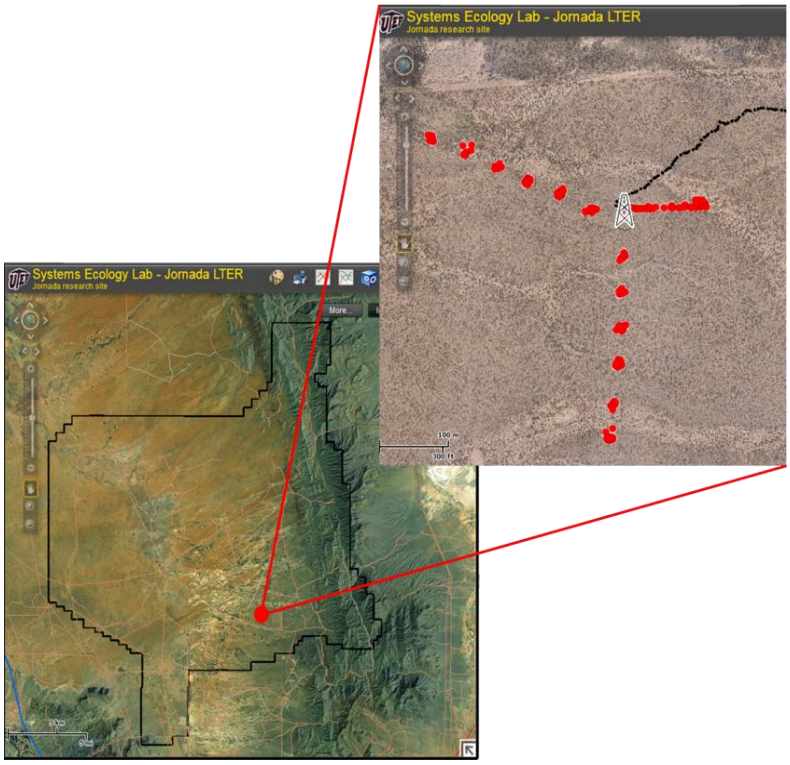

Figure 2.2 : Study site Latitude:32.581956, Longitude:-106.635025, located west of the San Andres Mountains on the JER at an elevation of 1188 m, and a moderate West facing slope of ~ 2 degrees. An interactive mapping application detailing the site can be found at (http://arctic.utep.edu/JornadaResearchFacility/).

2.1. CLIMATE

Climatic data for the Jornada Basin have been recorded since the 1920's and is available from the Long-Term Ecological Research (LTER) program, the USDA JER, the New Mexico State University Chihuahuan Desert Rangeland Research Center (CDRRC), and the U.S. Geological Survey (USGS). The JER is a Midlatitude (cold) desert (BWk) according to the Köppen classification (Havstad et al., 2006) , characterized by intense solar radiation, low relative humidity, high variability in annual precipitation, large ranges in diurnal temperature, and elevated rates of evaporation (evaporation exceeds precipitation) with a constant moisture deficit. Average precipitation for the Jornada Basin (1915 to 1995) is 245.1 mm. The lowest annual precipitation was 77.0 mm in 1953. The highest maximum rainfall documented was 507.2 mm in 1984 (Havstad et al., 2006). A pronounced wet season spans June to September and provides over the 50% of mean annual precipitation, with a peak in August. According to Havstad (2006), mean annual monthly temperature between 1915 and 1993 was 14.70°C with a standard deviation of 0.58°C. The mean monthly temperature for January was 6°C, and the mean monthly temperature for June was 26°C.

2.2. LANDSCAPE

The Jornada Basin Experimental Range ($783 km^2$) is located on La Jornada del Muerto Plain in the northern Chihuahuan Desert (Schmidt, 1979). Climatic fluctuations, topographic position, and parent material have influenced soil development since the Quaternary (Gile et al., 1981). This region has a gently sloping surface that is modified by wind, resulting in the formation of coppice dunes. Most dunes are on average 100 years old 4m in height, and 12m in diameter (Havstad et al., 2006). The Map by the Spatial Data Laboratory, USDA, ARS, and JER (2003) classifies the soil of the study area as "Soils of the valley border and piedmont slopes" (Ustic Calciargids) with a dominant

lithology of parent material composed of limestone and other sedimentary rocks, usually with some igneous.

2.3. VEGETATION

Plant communities in this region of the northern Chihuahuan Desert are classified as a desert-grassland transition (Havstad et al., 2006). Large expanses of Chihuahuan desert grasslands have been invaded by shrubs (Van Auken, 2000; Hochstrasser et al., 2002) and the majority of the northern Chihuahuan Desert is now dominated by desert shrublands (Gibbens et al., 1992; Peinetti et al., 2011). The invasion and increase in shrub density in former Chihuahuan Desert grasslands has been caused by numerous drivers acting concurrently and includes drought, livestock grazing, changes in fire regime, small animal activity, and changes in climate (Allred, 1996; Van Auken, 2000).

Jornada Experimental Range has been classified into five major vegetation types (Havstad et al., 2006): (1) Grasslands dominated by black grama (*Bouteloua eriopoda*), (2) Playa grasslands, (3) Shrublands dominated by tarbush (*Flourensia cernua*), (4) Shrublands dominated by creosotebush (*Larrea tridentata*), and (5) Shrublands dominated by mesquite (*Prosopis glandulosa*).

For this study, five key plant species that are relatively common throughout the Chihuahuan desert were selected for observation. These species are: honey mesquite *(Prosopis glandulosa),* creosote bush (*Larrea tridentata)*, tarbush (*Flourensia cernua)*, bush muhly (*Muhlenbergia porteri)* and fluff grass (*Dasyochloa pulchella)*. The following sections briefly describe biological characteristics of each species relevant to this study.

2.3.1 Honey Mesquite (*Prosopis glandulosa*)

Prosopis glandulosa is a deciduous shrub with a C3 photosynthetic pathway and is relatively long lived (ca. 200 years) (Fig. 2.3). This facultative phreatophyte has deep and extensive roots (Gibbens and Lenz, 2001). At the JER *P. glandulosa* occurs on most soil types, but is more common on sandy soils (Havstad et al., 2006). *Prosopis glandulosa* is a member of the Legume family (Leguminosae); acquiring most of their nitrogen from N-fixation (Geesing et al., 2000). *Prosopis glandulosa* grow up to 6 m tall, with one or two stout branches and spines, at each node. Leaves are alternate, and bipinnate. There is typically one paired division (pinnae) per leaf and 6 to 15 leaflets per pinna. Leaflets are 15 to 62 mm long and smooth (USDA NRCS National Plant Data Center). The flowers are arranged in axillary spikes that are 7 to 9 cm long and yellow or creamy in color. Each flower has 10 stamens and white ovaries. Seedpods are straight, about 7-20 cm long, reddish-brown, and between 6 to 6.5 mm long with brownish seeds (Havstad et al., 2006). *Prosopis glandulosa* may become invasive in some areas and may displace native and desirable vegetation if not properly managed (Hoffmann et al., 1993). The species is also highly tolerant of intense fires. Phenological observations of *P. glandulosa* are crucial to determine the timing of herbicidal application in population control applications because the phenological stage defines periods of vulnerability to herbicides. Typically this is approximately 40 to 60 days after bud break when leaves have reached full size, flowers are developed and small pods begin to form (Ansley et al., 2001). The timing when most deciduous species start their growing stage (e.g. open buds) is often influenced by winter temperature variability (Dokoozlian et al., 1999). Preston (1975) suggests that warm winters delay bud break for *P. glandulosa*, and that bud burst begins earlier under shaded areas of the canopy rather in zones exposed to direct sunshine. *Prosopis glandulosa* has undergone herbicide treatment in some areas of the Jornada but remains

widespread (Gibbens et al., 1993) occupying 95% of the Jornada in 1998 (Havstad et al., 2006). *Prosopis glandulosa* seed pods are consumed by jack rabbits, small mammals like kangaroo rats, and livestock, and various bird species nest on their branches.

2.3.2 Creosote Bush (*Larrea tridentata*)

Larrea tridentata is a multi-stemmed, evergreen C3 perennial shrub that is extremely resistant to drought and is long lived (up to 400 years) in the Chihuahuan Desert (Miller and Hunneke, 2000) (Fig. 2.4). Throughout the US desert southwest, *L. tridentata* is common (Reynolds, 1986) and is typically dominant on well-drained slopes and plains, especially where caliche is present. Soils where *L. tridentata* dominates typically have good drainage and are more porous than other soils (Smith et al., 1997). Its xerophytic tolerance is mostly due to physiological adaptations rather than morphological adaptations (Waide et al., 1999). *Larrea tridentata* typically has deep, non-overlapping root systems (Hamerlynck et al., 2000), and can photosynthesize throughout the year using soil water derived from either frontal storms or isolated summer rains (Franco et al., 1994). Furthermore, *L. tridentata* may have an effect on the survival and growth of other species (Peters, 2002). In general, shrub canopies can influence the interception, infiltration and storage of water, thereby resulting in an accumulation of nutrients under the shrubs, a phenomenon which has been analogously dubbed 'islands of fertility' (Whitford et al., 1996). Consequently soils underneath *L. tridentata* canopies are recognized to have higher concentrations of nitrogen than soils in the spaces between shrubs (Parker et al., 1982). Furthermore *L. tridentata* has an elevated tolerance to water stress and is capable of maintaining high net photosynthesis rates under water stress (Odening et al., 1974).

2.3.3 Tarbush (*Flourensia cernua*)

Flourensia cernua can grow up to 2m high, and is a deciduous C3 perennial shrub often found on sites that receive hydrological inputs from runoff (Fig. 2.5). In some situations, *F. cernua* can have a tar-like odor as a result of secondary compounds in its leaves (Estell et al., 1998). *F. cernua* has alternate, dark green leaves that are smooth, elliptic to pointed and 1.7- 2.5 cm long by 1 cm wide (Kingsbury, 1964; Powell, 1988). *Flourensia cernua* also has an extensive root system and is able to acquire both deep and superficial soil moisture (Gibbens and Lenz, 2001). Flower heads are yellow, small, solo, and not easily seen. The blooming period for *F. cernua* is in late spring. Plant communities where *F. cernua* is found are usually open, with a prevalence of bare ground, dispersed shrubs and grasses. *Flourensia cernua* tolerates flooding, but only for short periods of time (Dick-Peddie, 1993). Photosynthesis and transpiration from *F. cernua* increase rapidly in response to water availability (de Soyza et al., 2004).

2.3.4 Bush Muhly (*Muhlenbergia porteri*)

Muhlenbergia porteri is a C4 perennial grass that is usually found among boulders, cliffs, close to dry arroyos, and in grasslands. This species typically grows up to 25-100 cm tall (Fig. 8). It frequently occurs as clumps under shrub canopies (Dwight and Clark, 1975; Welsh and Beck, 1976; Chew, 1982), such as creosote bush and mesquite. *Muhlenbergia porteri* (Fig. 2.6) is consumed by livestock during winter when the availability of other grass species can be limited (Welsh and Beck, 1976). *Muhlenbergia porteri* can be susceptible to heavy grazing, because of its branching habit (U.S. Department of Agriculture, Forest Service; Welsh and Beck, 1976). *Muhlenbergia porteri* growth begins in late winter to early spring, and flowers in early spring to early summer (Kemp, 1983; Livingston et al., 1995). Dense growth of *M. porteri* may contribute to the spread of fire, especially when growing beneath shrubs.

2.3.5 Fluff grass (*Dasyochloa pulchella*)

Dasyochloa pulchella is a C4 perennial stoloniferous grass (Fig. 2.7), with an erect growth habit forming 4-10 cm long culms. It is typically found in rocky soils with open habitat (Pezzani et al., 2006). *Dasyochloa pulchella* belongs to the Chloridoideae subfamily (Clayton and Renvoize, 1986) and is a colonizing species with a relatively short-lived perennial life cycle (Pezzani et al., 2006). Foliage appears light green or purplish when young, and then turns to light green-white when mature, with 2-4 spikelets per branch. The "fluffy" appearance of the rosettes is apparent at maturity and is caused by fascicled spikelets with white hairs (Powell M., 2000).

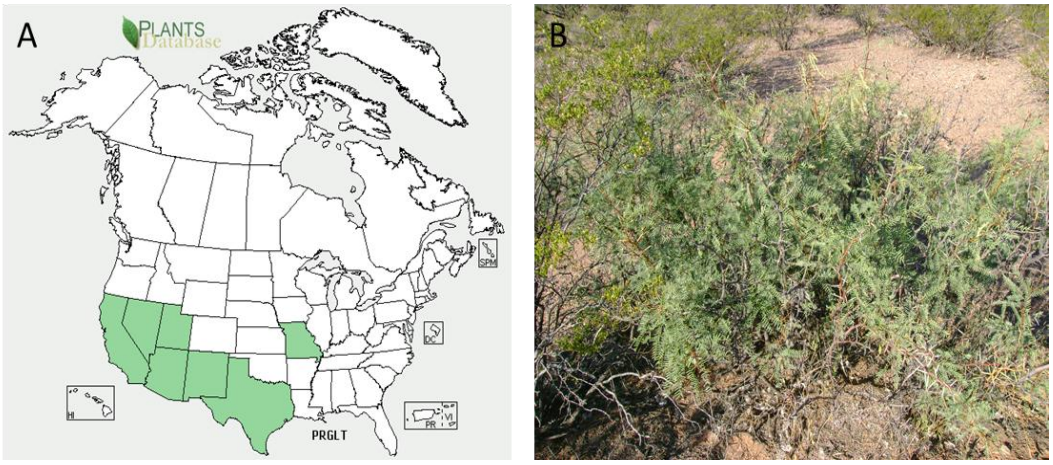

Figure 2.3: A-B. A. Distribution map on the U.S. of *P. glandulosa* (USDA Plants Database), B. *P. glandulosa* shrub in the Northern Chihuahuan Desert adjacent to creosote bush.

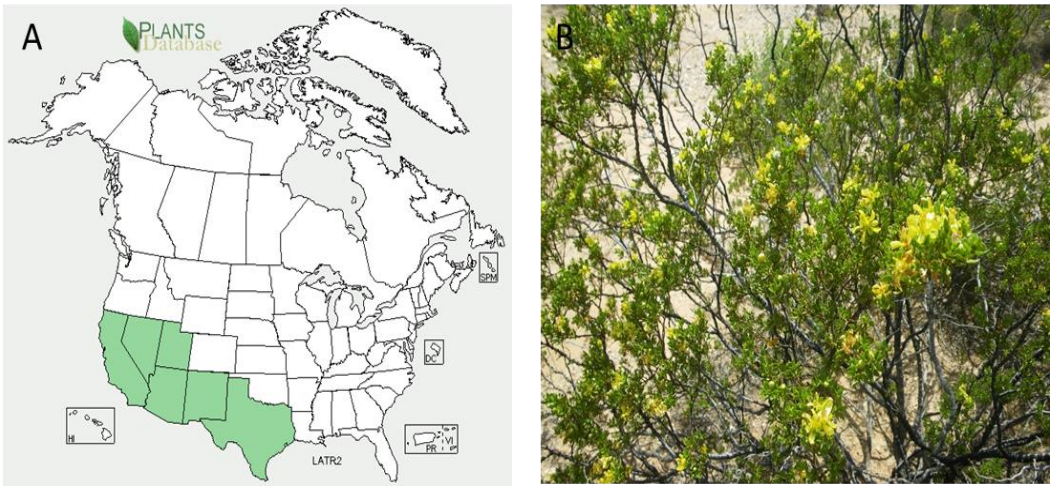

Figure 2.4: A-B. A. Distribution map *L. tridentata* in the US (USDA Plants Database). **B.** *L. tridentata* in full flower at the Jornada Experimental Range, May, 2010.

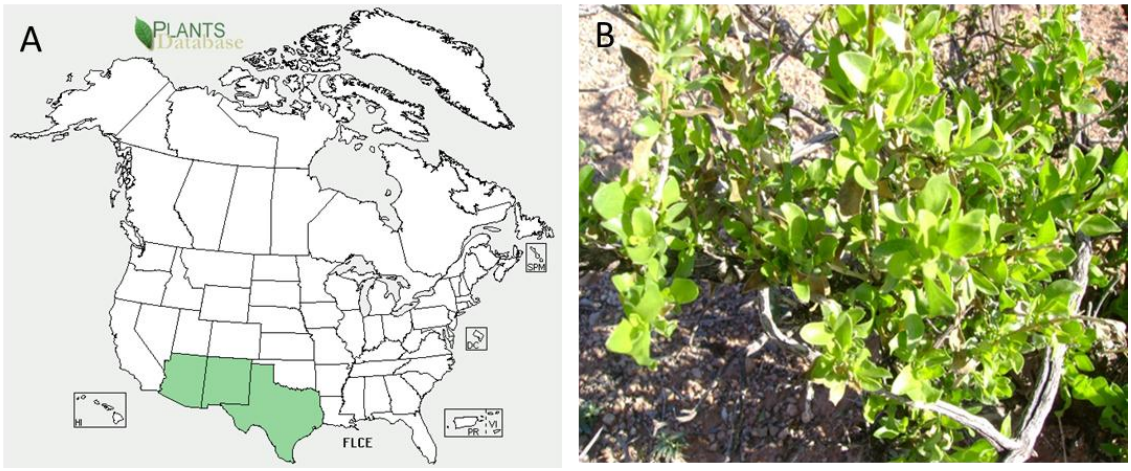

Figure 2.5: A-B. A. Distribution map of *F. cernua* in the United States (USDA Plants Database). **B.** *F. cernua* at full leaf size April, 2010.

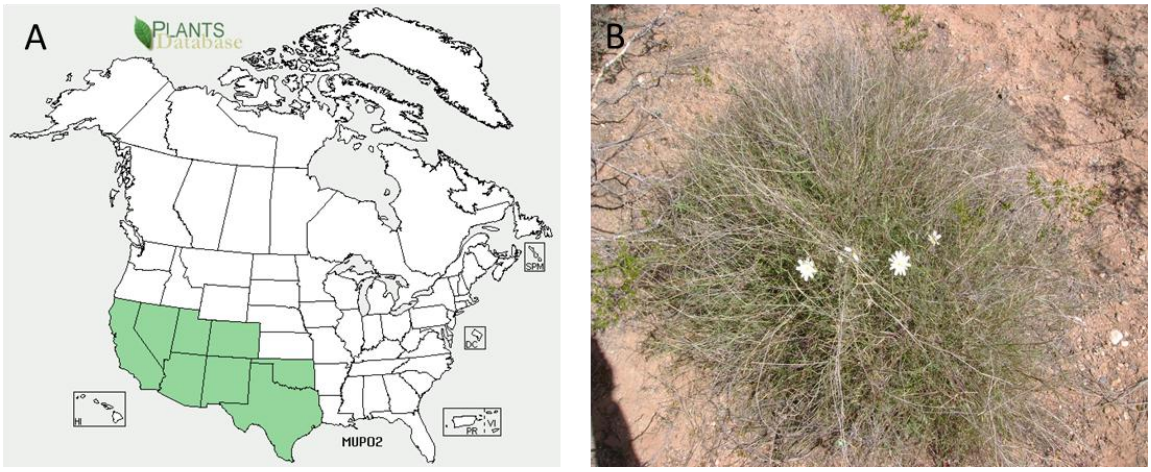

Figure 2.6: A-B. A. Distribution map of *M. porteri* in the United States (USDA Plants Database). **B.** *M. porteri* clump at the JER (April, 2010).

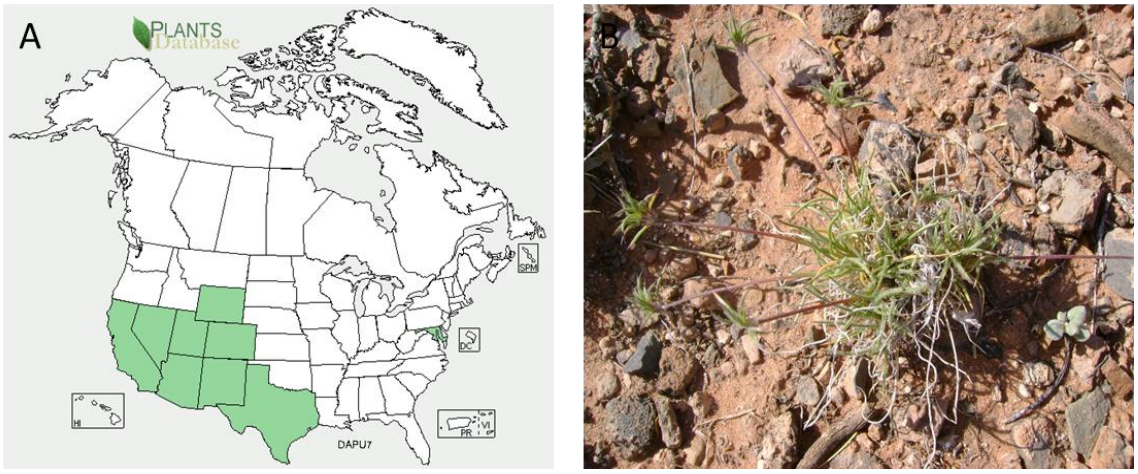

Figure 2.7:A-B. A. Distribution map of *D. pulchella* in the United States (USDA Plants Database). **B.** *D. pulchella* rosette along the East transect where weekly phenological observations were made.

2.4. HISTORY OF PHENOLOGICAL STUDIES

Many studies at the Jornada Experimental Range examine the causes and consequences of desertification (Havstad et al., 2006) to determine ecosystem dynamics across different ecological scales. Phenological studies have been conducted at JER since 1992, where monthly phenological observations are recorded at JER at each of the fifteen net primary productivity (NPP) sites. Numerous species are currently observed at each site and, species are monitored using different methods depending on abundance (line transect if abundant, or belt transect if scarce). Shrubs, perennial grasses and succulents are monitored to determine their reproductive status such as: dormant, vegetatively growing, budding, flowering, or in fruit. Long-term data on plant phenology is combined with simulation modeling output and remote sensing (Anderson et al., 2007) to characterize diverse landscapes at the Jornada Experimental Range.

Similar studies at the JER are relating field observations of plant phenological events to remotely sensed depictions of landsurface phenology (Browning, in progress) to monitor changes in land surface phenology, where the aim is to provide a basis for scaling relationships for phenology-based research applications. Duncan (1993) assessed the statistical relationships between spectral vegetation indices and semi-arid shrub cover at JER indicating the potential for the spectral differentiation of shrub types, and shrub from grasses, using multi-temporal, multi-spectral analysis. Bachelet (1988) quantified controls of environmental factors on phenological patterns of the northern Chihuahuan Desert, finding that annual plant phenology at JER can be predicted based on cues of rainfall, soil moisture, and temperature.

3. Methods

3.1. PHENOPHASE MONITORING

In March 2010 three phenology transects were established to monitor the foliar growth and reproductive phenological cycles of the five dominant perennial shrubs and grasses at the study site. Phenophase development was monitored weekly at sites along each transect. For the South and North-West transects (300m each) monitoring sites were situated every 50m (Fig. 3.1). Where possible, each site consisted of three tagged individuals of each of the five focal plant species (i.e. a maximum 15 tagged plants at each site). Some species were absent from some of the sites (see Table. 3.2) but all tagged individuals were found within 10 m of the site. The east transect was positioned parallel to the 110 m long robotic tram system oriented east-west downwind of the eddy-covariance tower. Along the east transect, ten individuals of each of the five focal plant species were tagged and monitored (see Table. 3.1). Where possible, plants were chosen and sampled from the boardwalk within the sampling footprint of the robotic tram system (see Section 3.4) to maximize the capacity for comparing results between instrument platforms and to limit surface disturbance near the tram system. Each individual was marked with a wooden peg painted with different colors that defined each species. The marker peg was tagged with a numbered aluminum swing tag. The choice of plants for phenological observation followed protocols developed by the US National Phenology Network USA-NPN (for additional information, see http://www.usanpn.org). The chosen plants appeared to be healthy, free from physical damage, and free of insect and fungal infection. The chosen plants also grew in similar environments each receiving the same amount of sun or shade, and were not in close proximity to other tagged plants of the same species. Protocols developed by the US-NPN were used for phenological observations (Figures: 3.2, 3.3, 3.4, 3.5 and 3.6). Because of the different plant

growth forms studied, not all phenophases were monitored for each species. Phenophases included categories for Leaf development (breaking leaf buds, leaves), flower development (open or unopened flowers), and the status of fruit (ripe or unripe fruits). On field data sheets modified from the US-NPN, the presence (Y) or absence of each (N) phenophase was recorded at each observation period for each tagged plant.

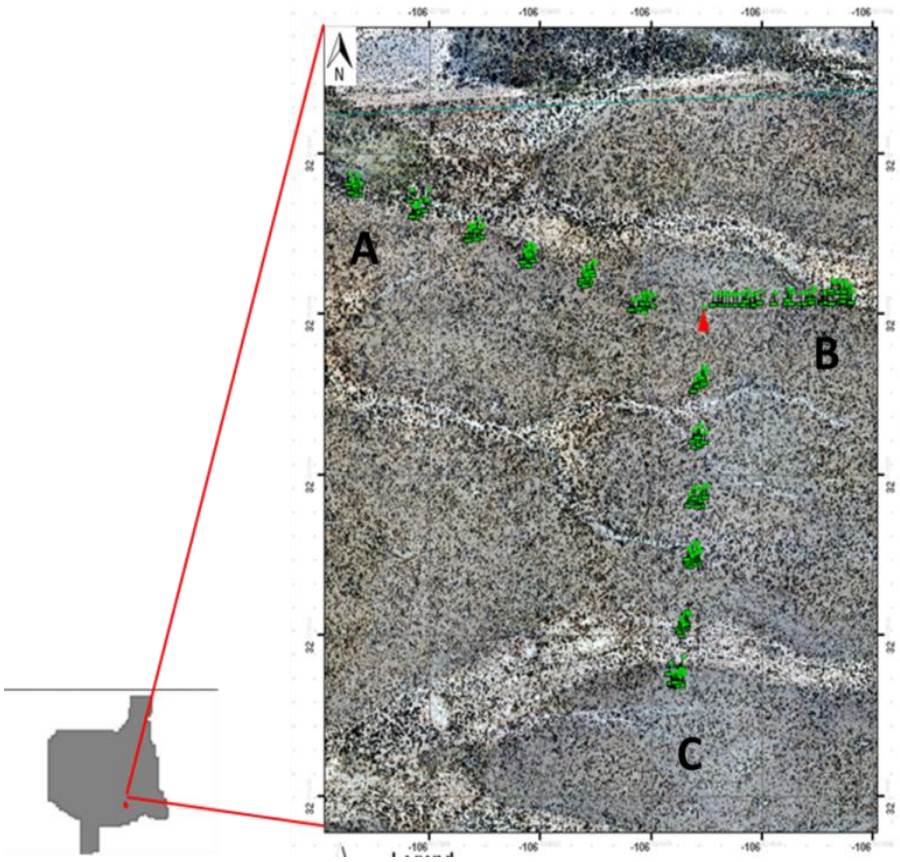

Figure 3.1: Phenology Transects (green dots indicate individually marked plants) situated at the study site **A**. North-West Transect **B**. East Transect **C**. South Transect. The North-West and South transects are 300m in length with monitoring sites situated every 50m. The East transect is situated along the 110m robotic tram system. Latitude 32.581956, Longitude -106.635025, Elevation 1188m and Slope 2 degrees.

Table 3.1 Focal plant species monitored for the phenology study. (Taxonomy derived from the *USDA (United States Department of Agriculture Plants Database* **http://plants.usda.gov/java/**)

Symbol	Scientific Name	Common Name	Family	Growth Habit	Duration
PRGL	*Prosopis glandulosa*	Honey mesquite	Fabaceae	Deciduous Tree/Shrub	Perennial
LATR	*Larrea tridentata*	Tarbush	Asteraceae	Deciduous Tree/Shrub	Perennial
FLCE	*Flourensia cernua*	Creosote bush	Zygophyllaceae	Evergreen Shrub	Perennial
MUPO	*Muhlenbergia porteri*	Bush muhly	Poaceae	Graminoid	Perennial
DAPU	*Dasyochloa pulchella*	Fluff grass	Poaceae	Graminoid	Perennial

Table 3.2 Number of individuals of each focal plant studied observed at each site and transect.

	South Transect						North-West Transect						East Transect	
Sites per Transect	6						6						1	Total Individuals per site
	Individuals per site													
Sites	1	2	3	4	5	6	1	2	3	4	5	6	1	
Prosopis glandulosa	3	3	3	3	3	3	3	3	3	3	3	3	10	46
Larrea tridentata	3	3	3	3	3	3	3	3	3	3	3	3	10	43
Flourensia cernua	0	3	2	3	3	3	0	1	0	3	3	3	10	46
Muhlenbergia porteri	3	3	3	3	3	3	3	3	3	3	3	3	10	46
Dasyochloa pulchella	3	3	3	3	3	3	3	3	3	3	3	0	10	34
Total individuals per site	12	15	14	15	15	15	12	13	12	15	15	12	50	**215**

Phenophases Monitored for Creosote Bush (*Larrea Tridentata)*

A 

Breaking leaf buds – 3.2A: Three or more breaking leaf buds are visible. For *L. tridentata* a leaf bud is considered breaking when a green leaf tip is visible at the end of the bud, but before the leaf has unfolded to expose the petiole. In Figure 10A the leaf bud is breaking from an internode on a stem.

B 

Young unfolded leaves - 3.2B: Three or more young unfolded leaves are visible. Once the petiole is visible, the leaf is considered young and unfolded. For *L. tridentata* young leaves have a brighter green color and are slightly glossier than mature leaves. If necessary, the leaf may be bent to see if the petiole is present.

C 

Open flowers - 3.2C: Three or more open and fresh flowers are visible. Flowers are considered open when reproductive structures are visible (e.g., pistils and stamens). Dry flowers should not count as open flowers.

D 

Full flowering – 3.2D: *L. tridentata* is considered in full flower when 90% or more of the canopy presents open flowers.

E 

Ripe fruits – 3.2E: Three or more ripe fruits are visible. For *L. tridentata* fruits are considered ripe when they are brown and open.

F 

Flower buds – 3.2F: Three or more flower buds are visible and flower buds have not yet bloomed into a full-size flower.

G 

Fruits developing – 3.2G: Three or more fruits are visible. For *L. tridentata* fruits are light green in color and have white hairs.

Figure 3.2: Creosote Bush (*Larrea Tridentata)* phenophases **A**. Breaking Leaf buds**, B**. Young unfolded leaves, **C**. Open flowers, **D**. Full flowering, **E**. Ripe Fruits, **F**. Flower Buds, **G**. Fruits

Phenophases Monitored for Honey mesquite (*Prosopis glandulosa*)

A 

Breaking leaf buds-3.3A: Three or more breaking leaf buds are visible. For *P. glandulosa* a leaf bud is considered breaking when a green leaf tip is visible at the end of the bud, but before the leaf has unfolded to expose the petiole.

B 

Young unfolded leaves-3.3B: Three or more young unfolded leaves are visible. Once the petiole is visible, the leaf is considered young and unfolded. If necessary, new leaves may be bent to see if the petiole is present.

C 

>25% of full leaf size-3.3C: A majority of leaves on the individual have not yet reached their full size and are still expanding.

D 

>75% of full leaf size-3.3D: A majority of leaves on the individual have almost expanded to their full size.

E 

50% of leaves fallen-3.3E: *P. glandulosa* is considered to have 50% of its leaves when half of the leaves have been dropped.

F 

All leaves Fallen-3.3F: When the individual has dropped all of its leaves.

G 

Open flowers-3.3G: Three or more open and fresh flowers are visible on the individual. Flowers are considered open when reproductive structures are visible (e.g. pistils and stamens). Persistent dry flowers should not be considered as open flowers.

H 

Full flowering-3.3H: *P. glandulosa* is considered in full flower when 90% or more of the canopy presents open flowers.

I 

Fruits-3.3I: Three or more fruits are visible. For *P. glandulosa* fruits are a long pod flattened with constrictions between seeds.

J 

Ripe Fruits-3.3J: Three or more ripe fruits are visible on the individual.

K 

Recent fruit drop-3.3K: when fruits or seeds have dropped or been removed, Do not include immature fruits that have dropped before ripening.

L 

Flower buds-3.3L: Three or more flower buds are visible. Flower buds have not yet bloomed into a full-size flower.

Figure 3.3: Honey mesquite (*Prosopis glandulosa*) phenophases. A. Breaking leaf buds, B. Leaves, C. >25% of full leaf size, D. >75% of full leaf size, E. 50% of leaves fallen, F. All leaves Fallen, **G**. Open Flowers**, H**. Full flowering**, I**. Fruits**, J**. Ripe fruits, **K**. Recent fruit drop, **L**. Flower buds.

Phenophases Monitored for Tarbush (*Flourensia cernua)*

A

Breaking leaf buds-3.4A: Three or more breaking leaf buds are visible on the individual. On *F. cernua* a leaf bud is considered breaking when a green leaf tip is visible at the end of the bud, but before the leaf has unfolded to expose the petiole see Figure A.

B

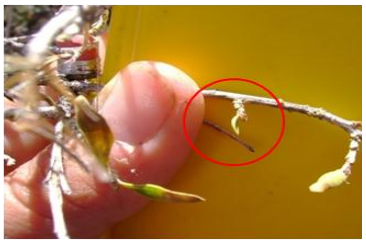

Young unfolded leaves-3.4B: Three or more young unfolded leaves are visible on the individual. Once the petiole is visible, the leaf is considered young and unfolded. If necessary, new leaves may be bent to see if the petiole is present.

C

>25% of full leaf size-3.4C: A majority of leaves on the individual have not yet reached their full size and are still expanding.

D

>75% of full leaf size-3.4D: A majority of leaves on the individual have almost reached their full size.

E

50% of leaves fallen-3.4E: P. glandulosa is considered to have undergone 50% leaf fall when half of the individual has dropped its leaves.

F

Flower buds-3.4F: Three or more flower buds are visible on the individual. Flower buds have not yet bloomed into a full-size flower.

Figure 3.4: Tarbush (*Flourensia cernua)* phenophases **A.** Breaking leaf buds, **B.** Leaves, **C**. >25% of full leaf size, **D**. >75% of full leaf size, **E.** >50 % of leaves fallen, **F**. Open flowers; Phenophases like: Full flowering, Fruits, Ripe fruits, and All leaves Fallen , were not recorded, because they did not appear on the individuals monitored.

Phenophases Monitored for Bush muhly (*Muhlenbergia porteri)*

A 

Initial growth-3.5A: New growth of the individual is visible, either as a new green shoot sprouting from a node on existing stems, or new green shoots breaking through the soil surface. For each shoot, growth is considered initial until the first leaf has unfolded.

B 

Leaves-3.5B: One or more live unfolded leaves are visible on the individual. A leaf is considered unfolded when it unrolls slightly from around the stem and begins to fall away at an angle. Dried or dead leaves should not be included in this estimate.

C 

All leaves withered-3.5C: When all of the leaves on the individual are dry, and dead.

D 

Flower heads-3.5D: One or more fresh inflorescences are visible on the individual. Inflorescence includes many small flowers arranged on spikelets, which emerge from inside the stem and gradually elongate with maturity. Flowers that have already opened or are dry should not be counted as flower heads.

E 

Open flowers-3.5E: One or more open fresh flowers are visible on the individual. A flower is considered open when reproductive structures (anthers or stigmata) can be seen protruding from spikelet.

F 

Fruits-3.5F: One or more fresh unripened fruits are visible on the individual

G 

Ripe Fruits-3.5G: One or more ripe fruits are visible on the individual.

Figure 3.5: Bush muhly (*Muhlenbergia porteri)* phenophases. **A**. Initial growth **B.** Leaves, **C.** All leaves withered **D.** Flower heads, **E.** Open flowers, **F.** Fruits, **G.** Ripe grains.

Phenophases Monitored for Fluff grass *(Dasyochloa pulchella)*

A 

Initial growth-3.6A: New growth of the individual is visible, either as a new green shoot sprouting from nodes on existing stems, or new green shoots breaking through the soil surface. For each shoot, growth is considered initial until the first leaf has unfolded.

B 

Leaves-3.6B: One or more live unfolded leaves are visible on the individual. A leaf is considered unfolded when it unrolls slightly from around the stem and begins to fall away at an angle. Dried or dead leaves should not be included in this estimate.

C 

All leaves withered-3.6C: When all of the leaves on the individual are dry, and dead.

D 

Flower heads-3.6D: One or more fresh inflorescences are visible on the individual. Inflorescences include many small flowers arranged on spikelets, which emerge from inside the stem and gradually grow taller. Flowers that have already opened or are dry should not be included in this estimate.

E 

Open flowers-3.6E: One or more open fresh flowers are visible on the individual. A flower is considered open when reproductive structures (anthers or stigmata) can be seen protruding from spikelet.

F 

Fruits-3.6F: One or more fresh fruits are visible on the individual

G 

Ripe Fruits-3.6G: One or more ripe fruits are visible on the individual.

Figure 3.6: Fluff grass *(Dasyochloa pulchella) phenophases*. **A**. Initial growth, **B**. Leaves, **C.** All leaves withered, **D**. Flowers heads, **E.** Open flowers, **F**. Fruits, **G**. Ripe fruits.

3.2. CLIMATE DATA

Phenological activity is influenced by several factors such as: light availability (Huete et al. 2006) temperature, moisture, and photoperiod (Rathcke and Lacey, 1985; Loomis and Connor, 1992; Kurc and Benton, 2010). Furthermore vegetation phenology in arid and semi-arid ecosystems is primarily controlled by water availability (Zhang et al., 2005), triggering the emergence of green leaves and controlling vegetation growth duration (Peñuelas, 2004). The study site has an open path Eddy Covariance tower where environmental measurements are made at high frequency. These measurements include precipitation, air temperature, relative humidity, wind speed, photosynthetic active radiation (PAR) and others. Creating a link between plant phenology development, and meteorological data for a better understanding of key phenological events is crucial. Hence this study analyzes phenological response to environmental cues at the JER by the integration of "near-remote sensing" techniques.

A 10-m tall tower hosting an open path eddy covariance (OPEC) system designed to measure land-atmosphere flux exchange was deployed in November 2009. The OPEC provides digital output of the fluctuations of carbon dioxide (CO_2) density, latent heat, sensible heat, momentum, temperature, humidity, horizontal wind speed and wind direction, net radiation, soil heat, soil temperature, and soil water content (Campbell Scientific, 2009). The system was designed following standard protocols of national and international networks (FLUXNET, AMERIFLUX), and also matched other sites with OPECs in the US southwest. Manufactures protocols were followed for sensor installation, maintenance, and calibration (Campbell Scientific, 2004-2006; Kipp & Zonen 2004; Decagon 2007; LICOR 2007). Every season the CO_2 signal of the IRGA is calibrated against gas mixtures with a 500ppm CO2 concentration; the range for water vapor is calibrated

with a dew point generator model Li 610, Li-COR Inc. Zero spans for both CO_2 and water vapor channels are calibrated with 99.99% nitrogen gas.

Adhering to the AMERIFLUX protocol 30 min fluxes are calculated from fast response instrumentation, and independent measurements from slower response sensors are used to measure and calculate background meteorological variables. The (OPEC) tower has a total of 22 instruments (Fig. 3.7 - numbers for the following refer to numbers given in Fig. 3.7.): three dimensional sonic anemometers (4), an infrared gas analyzer (5), a four component net radiometer (3)(CNR1- Kipp and Zonen), a photosynthetically active radiation sensor (2) (PAR-LITE - Kipp and Zonen), soil heat flux plates (10) (HFP01 Hukseflux), a temperature and humidity sensor (8) (HMP45C-L - CSI), a barometric pressure sensor (9) (CS106 –CSI), a wind speed and direction sensor (1) (03002-L -CSI), a soil temperature and volumetric water content sensor (11) (ECTM – decagon), a precipitation sensor (7) (TE525-L tipping bucket), and two leaf wetness sensors (LWS decagon). All the data are stored in a Campbell Scientific CR3000 datalogger. The system is powered with a 500W 10 solar panel array. The solar panels are mounted on an aluminum structure located 35m north from the (OPEC) tower. The panels have a clear view of the southern horizon to maximize battery charging. The system uses four 12VDC sealed deep cycle batteries, and the load is regulated through a morning start ProStar 15 Amp 12/24 charge controller. Two GB data storage cards are exchanged on a weekly basis. Additionally, data are retrieved remotely using an internet connection provided by the JER headquarters. The signal is sent and received by two antennas (bidirectional and omnidirectional) one located at 9m and the other at 5m height from the (OPEC) tower. The system also has a 500m radio WI-FI bubble to operate other wireless sensors (Jaimes, in preparation).

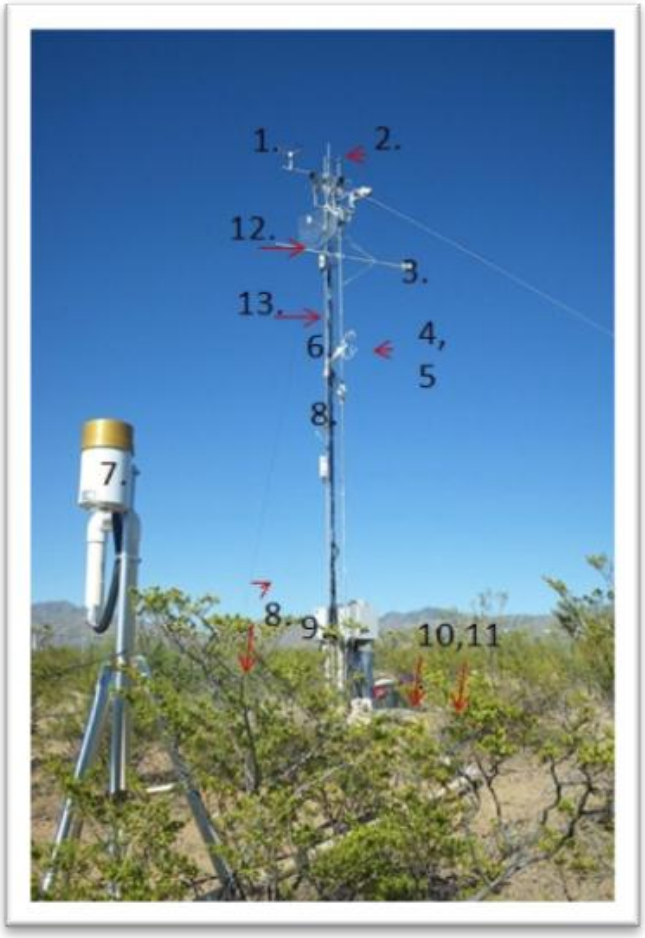

Figure 3.7. Eddy Covariance tower Instrumentation: (1) wind speed and direction , (2) photo synthetically active radiation, (3) four component net radiometer, (4) three dimensional sonic anemometers, (5) infrared gas analyzer, (6) IRGA, (7) (ECTM – decagon), precipitation, (8) temperature and humidity, (9) (HMP45C-L - CSI), barometric pressure, (10) CNR1- Kipp and Zonen), (PAR-LITE - Kipp and Zonen), and soil heat flux plates, (11) (HFP01 Hukseflux), (CS106 –CSI), (03002-L -CSI), soil temperature and volumetric water content (TE525-L tipping bucket), and two leaf wetness sensors(LWS decagon) .

3.3. DEVELOPMENT, TESTING, AND ANALYSIS OF DIGITAL PHENOCAMS

To choose an optimal web cam for phenophase monitoring, the optical and other properties from four different models of camera from three different manufacturers were compared (see Table 3.3). The Green Roof of the Biology Building at The University of Texas at El Paso (UTEP) was utilized for initial image acquisition and testing. Each camera was centered on the same region-of-

interest (ROI), so the spectral properties of each camera could be compared. To differentiate changes in canopy state (Fig. 3.8) the size of the ROI was normalized to Y 300, X 500 pixels respectively for all images. Spectral properties of each camera were compared using the image acquisition tool box of Matlab 7.8.0 (R2009a; The Mathworks). Similar to Richardson et al. (2007), the channels for Red, Green, and Blue (RGB) were extracted from the standardized ROI for each image taken by each camera. The overall brightness (Total RGB) from the ROI was calculated using Equation 1 (below) and used to calculate the relative (or normalized) brightness for each channel using Equation 2 (below). The greenness index formulated by Richardson et al. (2007) is given in Equation 3 (below). This is the same as the index *Ig* used by Kurk and Benton (2010).

$$Total\ RGB = Red + Green + Blue \quad (1)$$

$$Relative\ Channel\ brightness\ (\%) = \frac{Channel}{Total\ RGB} \quad (2)$$

$$Greenness\ Index\ 2\ x\ (Green) - (Red + Blue) \quad (3)$$

Table 3.3 Relevant specifications of the four webcams tested in this study

Camera	Max resolution	View angle	Focus	Max fps	Interface	Sensor	Price	Lens	Pros	Cons
Logitech Quickcam Af	1600x1200	58°	auto	30	usb 2.0	CCD	$129.00	glass	motorized pan-tilt	bad image quality
Micrsoft Vx6000	1280x1024	71°	manual	30	usb 2.1	CCD	$40.00	Plastic	wide angle	plastic lens cause circular patterns
Micrsoft Vx7000	1600x1200	58°	fixed	30	usb 2.2	CM 05	$45.00	glass	clear images	no manual focus
Canon sd870	3264x2448	60°	auto	30	SD memory card	CCD	$279.00	glass	high quality images	no computer user interface

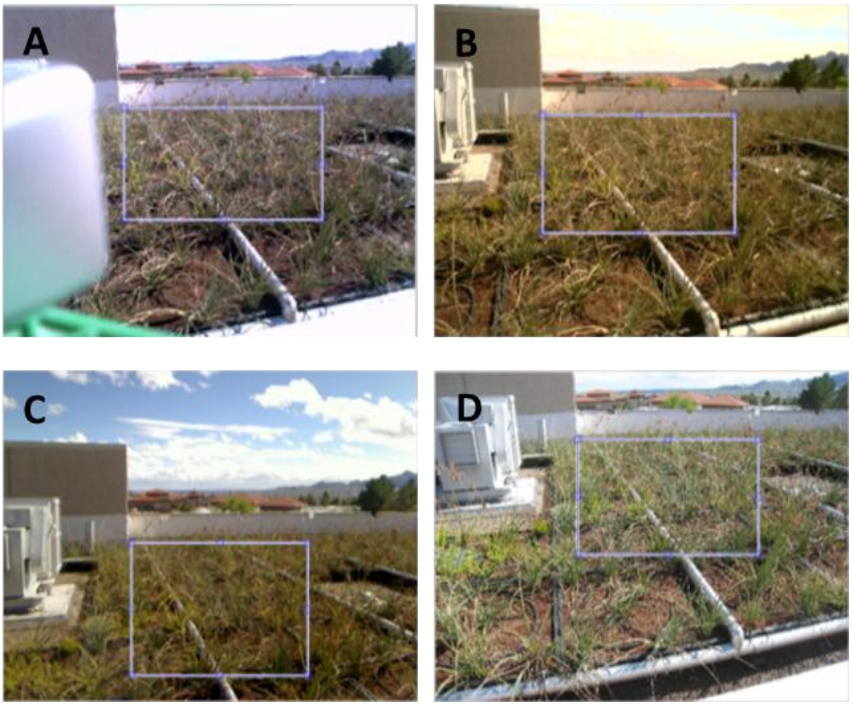

Figure 3.8: A-D. Webcam images taken with each of the four webcams tested for a similar region of interest. **A**. Microsoft Vx6000**, B**. Logitech, **C**. Microsoft Vx7000, **D.** Canon sd870. Tests of the webcams were made at UTEP's green roof on the Biology building.

The Microsoft webcam model Vx7000, with 1600 x 1200 pixel resolution (2 MP), 58° of horizontal view angle, with a manually fixed focus for the specific experimental area (The Eddy Covariance tower's footprint), was the best camera suited for this study according to our evaluation criteria. Features of the camera demonstrate that this visual instrument optimizes the recording of phenological stages and detects spatial and temporal variation, by RGB channel extraction in a cost effective way.

To determine the amount of variability between different Vx7000 webcams, four of the Vx7000's were mounted in a customized weatherproof camera enclosure and connected to a Belkin USB Plus 4-Port Hub (5V/2.6 A), , with a 36ft Tripp Lite U042-036 USB2.0 A/B repeater cable extension (Fig. 3.9). The hub was connected to a laptop computer, which ran a Matlab 7.8.0 (R2009a; The

Mathworks) image acquisition routine. The acquired images were stored with a minimal compression factor in JPEG format.

Using the green roof at the Biology building at the University of Texas at El Paso, images from each camera were compared to assess the degree of variability among cameras by selecting a similar ROI (Fig. 3.10) and extracting the relative channel brightness for each. The cameras demonstrated a relatively low degree of variability between cameras (Fig. 3.11), suggesting that multiple cameras of this model were capable of acquiring repeat and comparable images suitable for analysis of landscape phenology.

Although the analysis of digital images has become widely used for phenological analysis, there is no standardized software for controlling image capture and analysis. To acquire process and analyze digital imagery a software plugin was developed for Matlab 7.8.0 (R2009a; The Mathworks). A graphical user interface (GUI) was also developed in collaboration with graduate students at UTEP's Cyber-ShARE Center of Excellence to define the capturing schedules and permit selection of ROIs for analysis using Equations 1-3 above (Fig. 3.12).

To capture landscape phenology at the JER field site, four cameras were established 9m above ground level on the Eddy Covariance tower. One camera was pointed at 58° northeast to capture the tramline study area. The remaining three cameras were pointed towards the dominant footprint of the eddy tower. Images spanned a 170° radial view angle and overlapped slightly in their coverage. Cameras were programmed to acquire images hourly between 7:00- 19:00 each day. Images captured were uploaded to Picassa via the point to point wireless internet connection between the site and JER headquarters.

To establish ROIs for spectral analysis and to maximize comparison among photographs, constant distances away from the main eddy tower were photographed (15m, 50m, 180m, 450m, and 500m, see Fig. 3.13), which allowed for ROIs with a similar distance to the eddy tower to be identified for each of the scenes captured by the webcams. The footprint of the eddy covariance measurements is highly dynamic and varies from to more than 600m from the tower. To capture this variability and maximize the amount of vegetation captured in a given scene, an ROI for each of the three cameras was set to span 180-500m from the tower. For the webcam covering the tramline, an ROI corresponding to the footprint of the tram measurements was established.

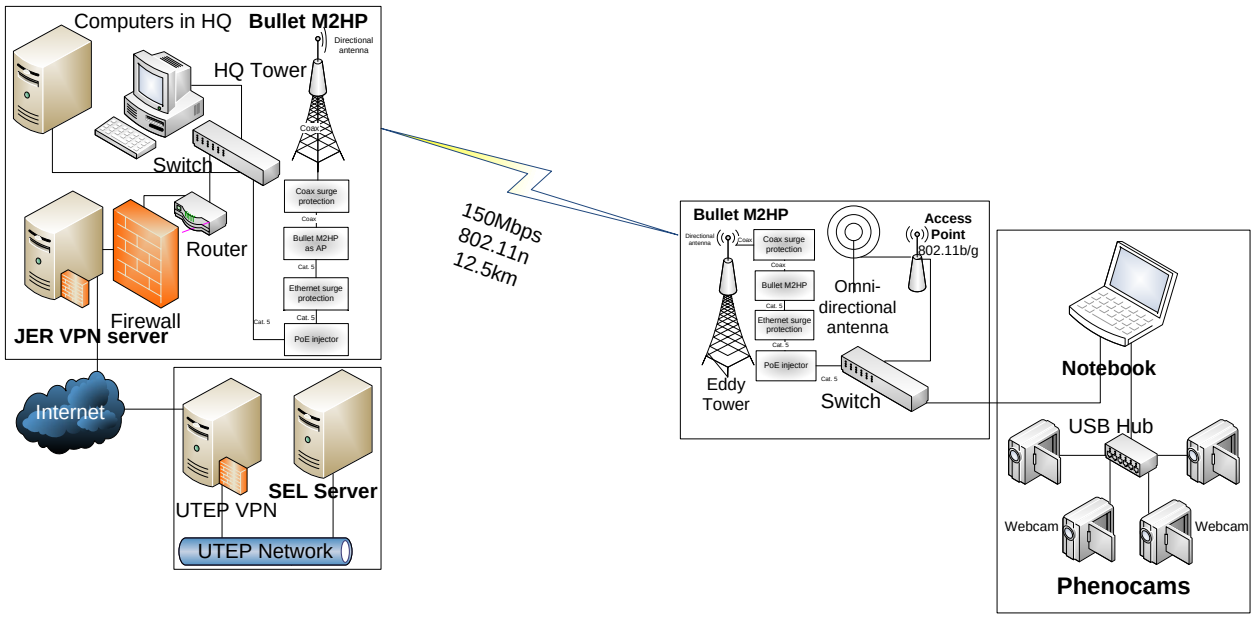

Figure 3.9: Schematic describing the communications system for the JER experimental infrastructure (courtesy of Gesuri Ramirez). Webcams are connected to laptop computer through a USB, and images are uploaded to Picassa via the point to point wireless internet connection between the site and JER headquarters, allowing access to servers at UTEP

Figure 3.10: Comparison between the four Microsoft Vx7000's to assess the degree of variability between cameras by selecting a similar ROI, made at the green roof at the Biology building at the University of Texas at El Paso

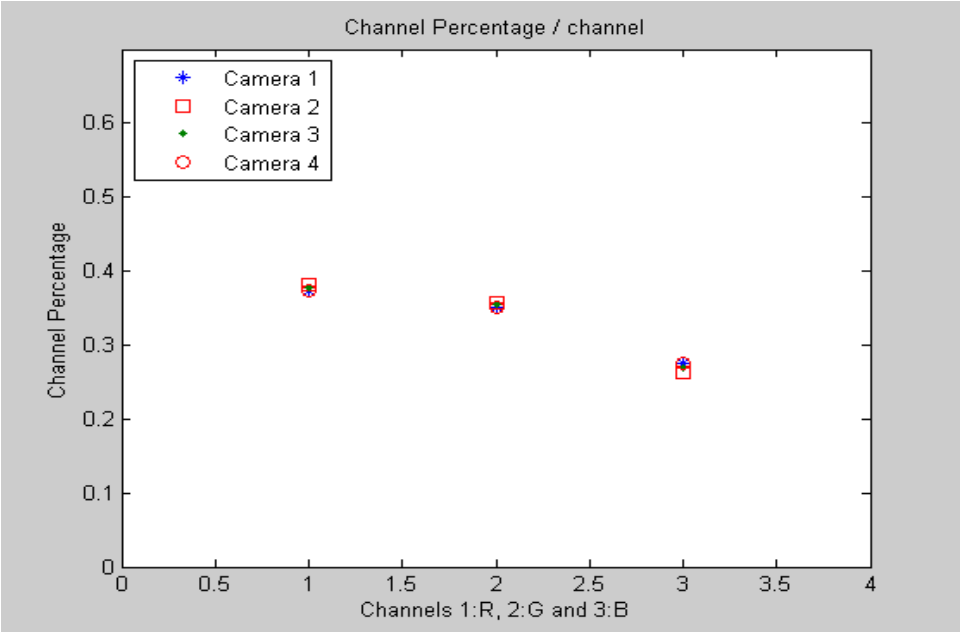

Figure 3.11: Results from channel brightness analysis of the four VX7000 Microsoft webcams. All four cameras showed remarkably similar and repeatable spectral signatures for same ROI.

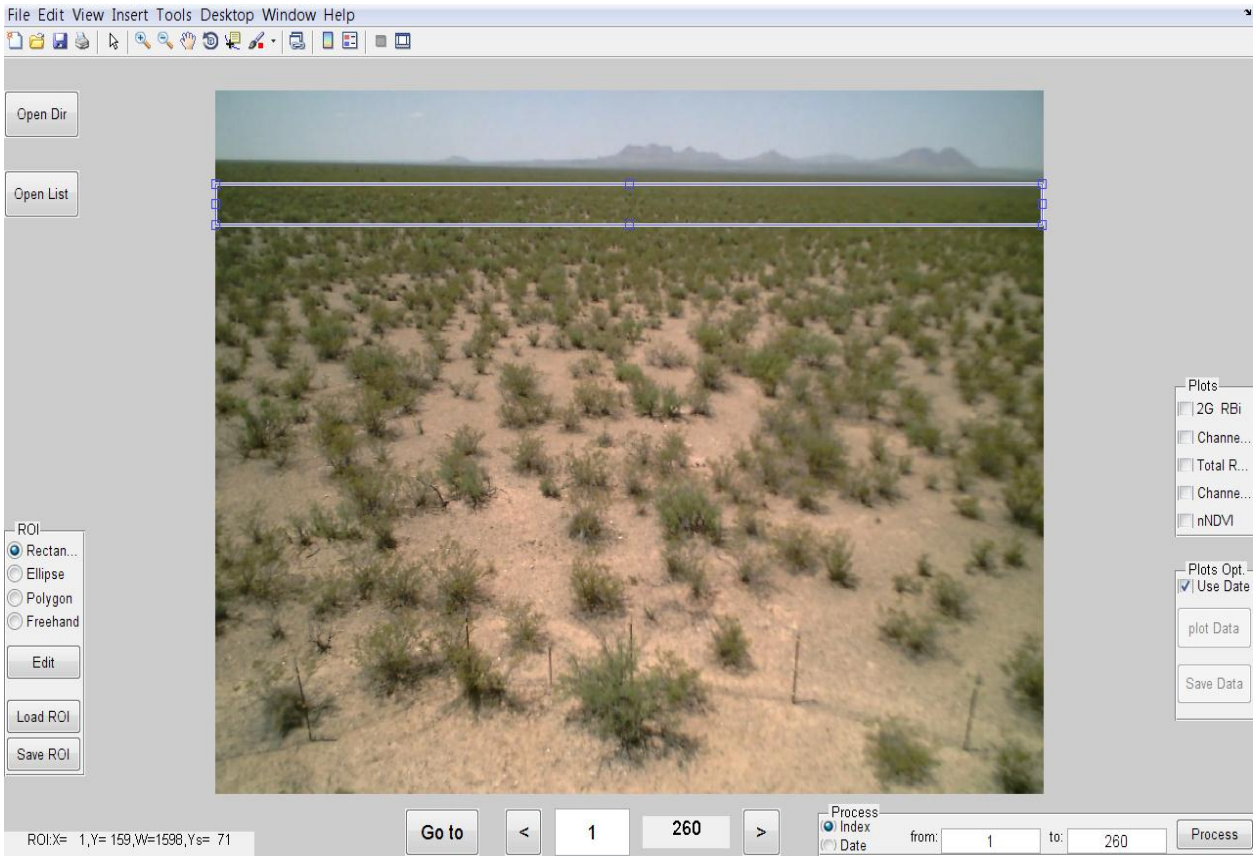

Figure 3.12: Graphical user interface for the MATLAB plugin developed for ROI selection and scheduling image acquisition. User interface for (ROI) selection and scheduler setup.

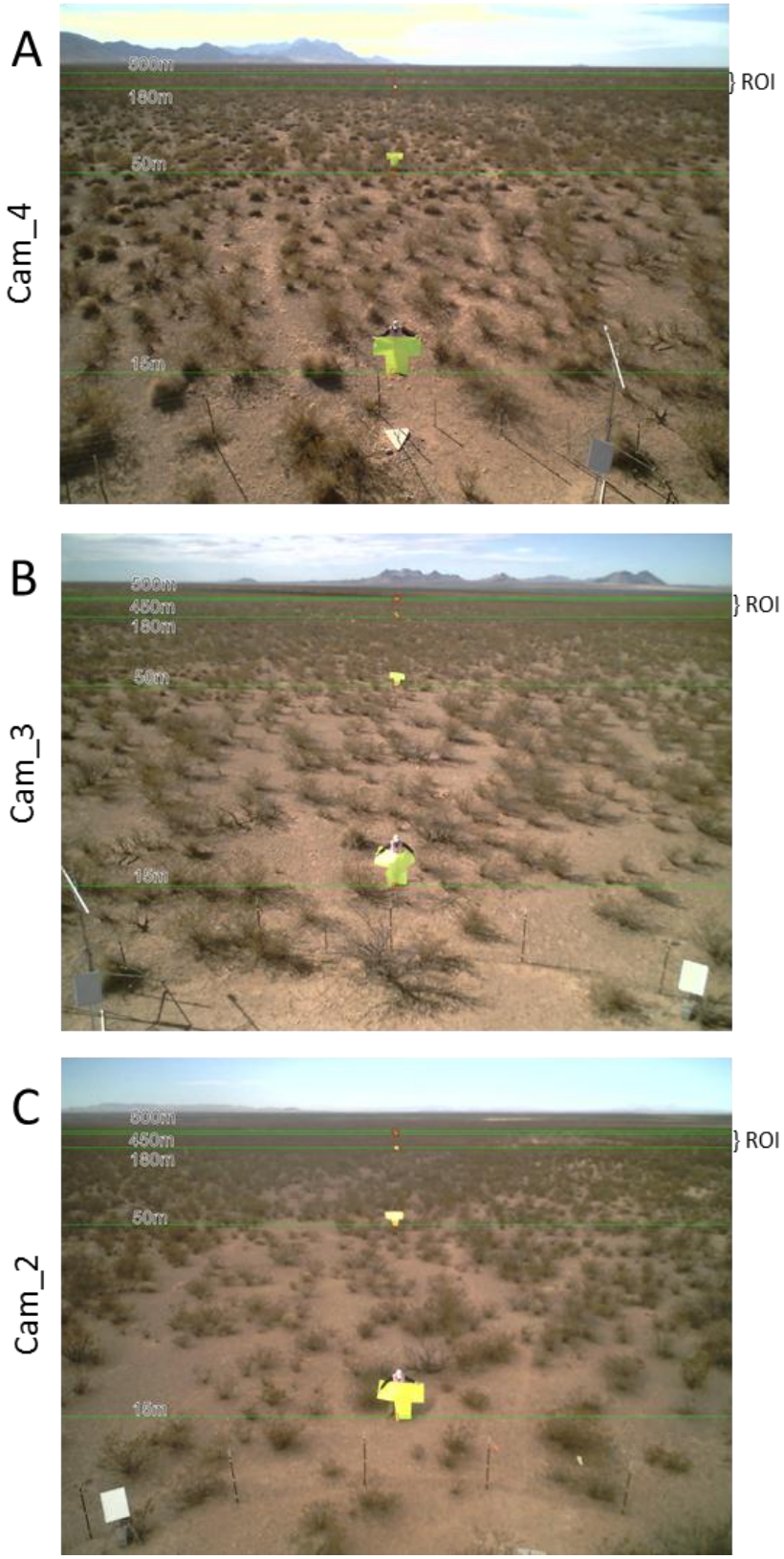

Figure 3.13: Establishing ROIs for each of the webcams imaging the footprint of the eddy covariance tower. ROIs are given for 180-500m from the tower in the south facing web cam (A), southwest facing webcam (B), and west facing webcam (C).

3.4. ROBOTIC TRAM MEASUREMENTS

Efficient, repeat measurement of vegetation phenology over landscape to regional scales requires analysis of imagery acquired from satellite based sensors. There is a need, therefore, to correlate greenness indices derived from the webcams with greenness indices derived from sensors that can duplicate the spectral properties acquired by satellite platforms. The JER study site is an excellent study area to do this because it is the only site we are aware of in a desert location where plant phenophase development, micrometeorology and carbon, water and energy fluxes are being measured simultaneously and in an integrated way.

This study compares phenology measurements made with the phenocams described above with greenness derived from the robotic tram system, which is used to measure hyperspectral reflectance. The robotic cart used in the tram system is equipped with a dual-detector field portable spectrometer (Unispec DC, PP Systems, Amesbury, MA, USA). The spectrometer collects both radiance data (radiation from the surface target) and irradiance data (radiation from the sky) simultaneously, which permits correction of surface reflectance under changing sky conditions. The spectrometer undergoes two calibrations necessary to yield accurate field data collection. At the start of a data collection session, a dark calibration is performed and then cross-calibrated with a 99% reflectance white panel (Spectralon, Labsphere, North Sutton, NH, USA) at the beginning and end of each sampling run along tramline. The Unispec DC operates at a spectral range of 303 and 1148 nm in 256 contiguous bands.

At the JER study site, the robotic cart traverses a 110 m long transect (an elevated and leveled tramline) east and most often downwind of the eddy-covariance tower. The tram system is oriented in an east-to-west direction and all spectral measurements are made on the south side to minimize shading. Along the rail trigger marks are situated every meter. These activate a

mechanical switch mounted on the base of the robotic cart as it passes by that meter-mark, causing the spectrometer to make a measurement. As the cart reaches the end of the tram rail, a crossbar on the rail activates a different switch mounted on the cart that reverses the polarity of the electric engine and reverses direction. More information on the development and testing of the tramline can be found in Gamon et al. (2006) and Goswami et al. (2011).

The robotic tramline is operated once per week within a few hours of solar-noon to avoid shading. Reflectance data was processed using the software Multispec version 5.1 which interpolates reflectance values to 1nm reflectance intervals between 400 and 1148nm. For this study, the greenness index NDVI (normalized difference vegetation index) was calculated using Equation: NDVI=(R800 – R680)/(R800 + R680), where R680= reflectance at 680nm, and R800= reflectance at 800nm. As well as acquiring measurements of hyperspectral reflectance, the tram system was used to acquire digital imagery at every meter each time the robotic tramline was operated. The imagery was acquired using the same brand and model of webcams mounted on the eddy covariance tower. Digital imagery was processed using Matlab 7.8.0 (R2009a; The Mathworks) software described above. This software allowed for a circular ROI to be established, which matched the sampling footprint of the Unispec. The tram NDVI and greenness index derived from digital images were compared for the tramline as a whole, and for bare ground and each species of plant sampled at each meter of the tramline.

4. Results

4.1. PHENOPHASE MONITORING

For 14 months, weekly observations of phenophase development were made for five dominant species at the study site. Phenophases that were monitored for frequency of occurrence and included the following phenophases: breaking leaf buds, live leaves, all leaves fallen (shrubs), all leaves withered (grasses), flower buds, open flowers, fruits (shrubs), grains (grasses), ripe fruits and grains. Phenophase development did not appear to differ between the three transects monitored so data was lumped and has been presented as a mean frequency of occurrence for each phenophase for each day of observation. Overarchingly, results reflect substantial differences in phenophase development between species for each phenophase category monitored.

For the phenophase category breaking leaf buds, *L. tridentata* presented breaking leaf buds throughout the study period, except following the February 2011 freeze event where breaking leaf buds died on 74% of the individuals studied (Fig. 4.1). Breaking leaf buds on *M. porteri and D. pulchella* were initiating as phenophase measurements began on day 68 of 2010 and extended through day 187 (M. porteri) and day 152 (*D. pulchella*) in 2010. Of all the species studied *M. porteri* followed by *D. pulchella* had the longest period with breaking leaf buds in 2010, with the exception of *L. tridentata*. For both *M. porteri* and *D. pulchella*, the onset of breaking buds was not observed in the 2011 study period and was at least 50 days later in 2011 than in 2010. For *F. cernua* breaking leaf buds were first recorded on day 75 of 2010 and ceased by day 117. *Prosopis glandulosa* was the last species to initiate leaf buds and began on day 96 of 2010. *Prosopis glandulosa* was the only species other than *L. tridentata* to initiate leaf buds in 2011 but the first observations in 2011 were on day 119, 23 days after the initiation date recorded for 2010. The phenophase class “live leaves” is given for each of the five plant species studied in Figure 4.2.

Dasyochloa pulchella and *M. porteri* were the first species to display leaves initiating on day 70 of 2010. This was followed by *F. cernua* on day 82 of 2010 and extended throughout day 138 of 2010. Day 96 was the first day when leaves were recorded for *P. glandulosa* in 2010 and day 119 for 2011. Of all the species studies, *D. pulchella* followed by *M. porteri* had the longest period with leaves in 2010, with exception of *L. tridentata* which presented leaves throughout the study period, except following the February 2011 freeze event. The phenophase "flower buds" is given for each of the five plant species studied in Figure 4.3. *Dasyochloa pulchella* and *P. glandulosa* were the first species to initiate flower buds beginning on day 110 of 2010. For *L. tridentata* flower buds were first recorded on day 117 of 2010 and ended on day 152 of 2010. *Muhlenbergia porteri* was the last species to initiate flower buds in day 223 of 2010. *Dasyochloa pulchella* had the longest period with flower buds of all the species studied. For *F. cernua* the onset of flower buds was not observed in the study period.

The phenophase "open flowers" is given for each of the five plant species studied in Figure 4.4. Open flowers on *P. glandulosa* and *L. tridentata* initiated on day 131 of 2010 and extended through day 159 (*P. glandulosa*) and day 208 (*L. tridentata*). For *D. pulchella* open flowers were first observed on day 236 of 2010 and ended by day 292. *Muhlenbergia porteri* had the longest period with open flowers in 2010 initiating on day 223 and ceasing by day 292. For *F. cernua* open flowers were not observed in the study period. The phenophase "fruits" is given for each of the five plant species studied in Figure 4.5. Fruits were first observed for *L. tridentata* initiating on day 138 of 2010 and ceased on day 286 of 2010 having the longest period with fruits in 2010. For *P. glandulosa*, fruits were initiated on day 159 of 2010 with only 28% of individuals studied fruiting. For *M. porteri* fruits started appearing on day 229 of 2010 and extended throughout day 272 of

2010. For *D. pulchella* fruits phenophase initiated on day 250 of 2010 and ended on day 292 of 2010. For *F. cernua* fruits were not observed in the study period.

The phenophase "ripe fruits" is given for each of the five plant species studied in Figure 4.6. *Larrea tridentata* was the first species to initiate ripe fruits, beginning on day 152 of 2010 and ceased on day 59 of 2011 having the longest period of ripe fruits of all the species studied. *Prosopis glandulosa* ripe fruits were initiated on day 223 of 2010 and extended until day 286 of 2010. For *M. porteri* ripe fruits initiated on day 250 of 2010 followed by *D. pulchella* on day 258 of 2010. For *F. cernua* ripe fruits were not observed during the study period. The phenophase "all leaves fallen/withered" is given for each of the five plant species studied in Figure 4.7. Leaf withering initiated for *D. pulchella* on day 138 of 2010 and day 278 for *M. porteri*, both of them remaining on a dormancy stage throughout the rest of the study. For *P. glandulosa* and *F. cernua* all leaves fallen were first recorded on day 314 of 2010. *Prosopis glandulosa* was the only species that came out of the dormancy stage on day 119 of 2011 with the exception of *L. tridentata*.

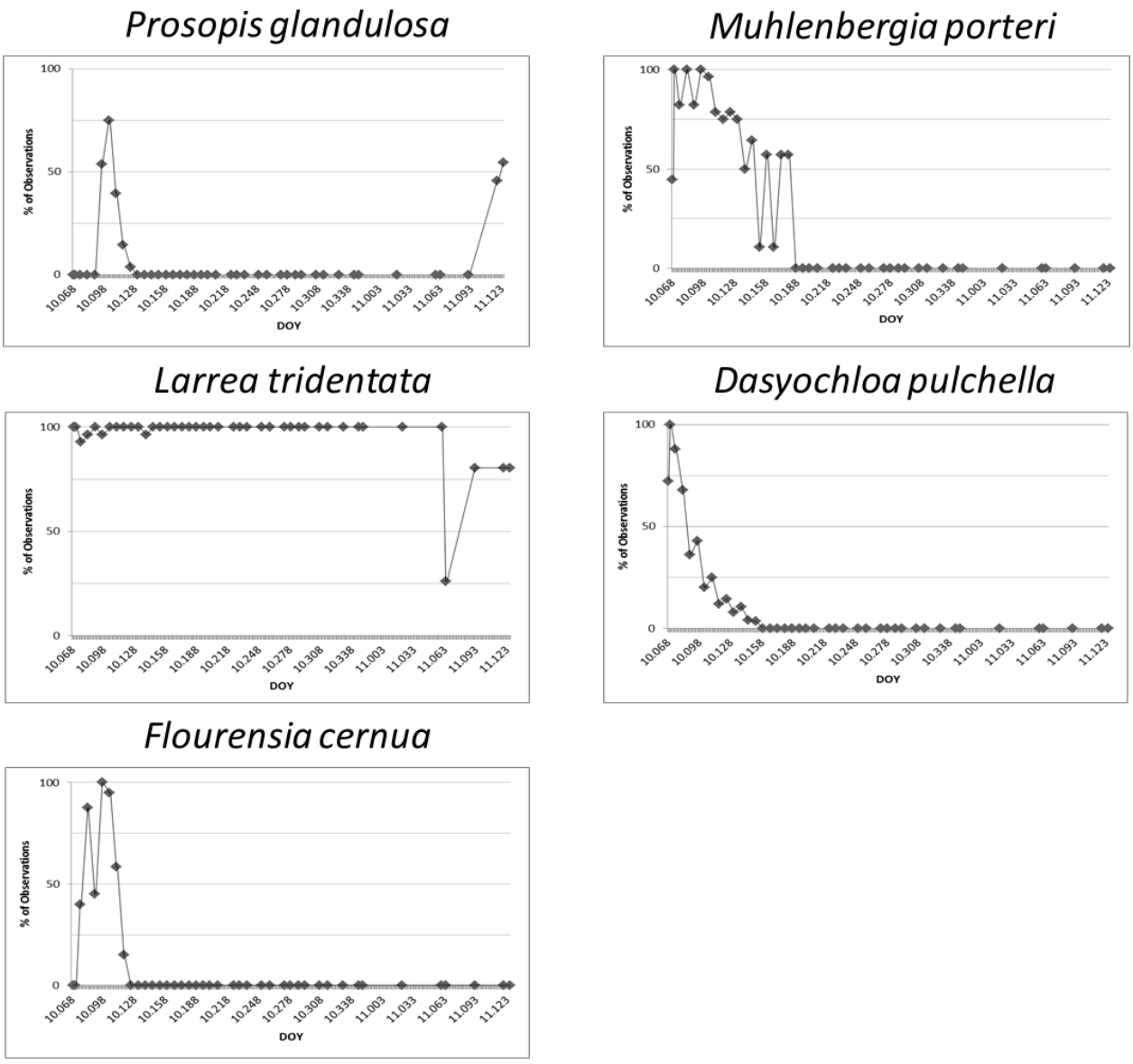

Figure 4.1: Phenological observation for breaking leaf buds

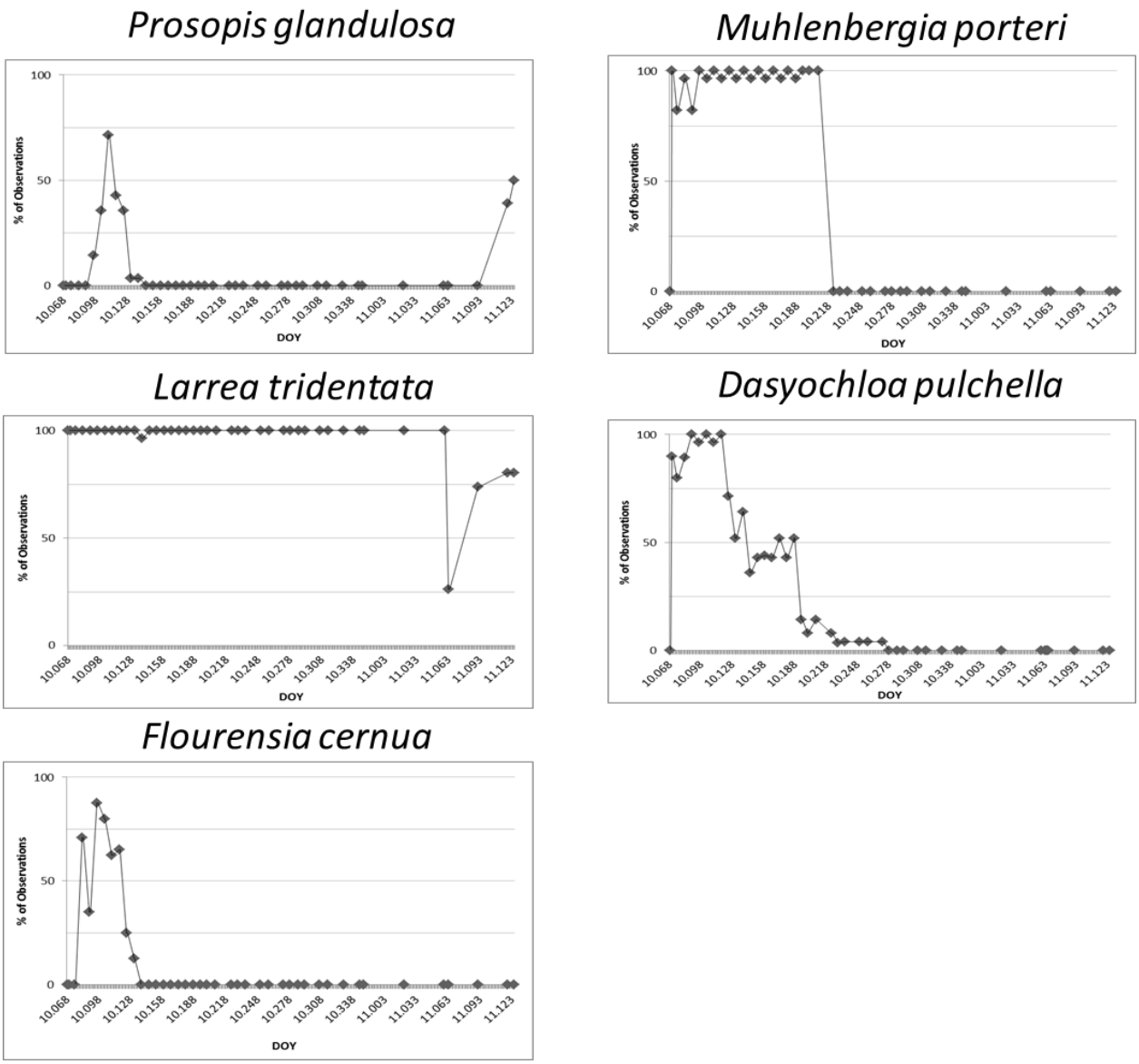

Figure 4.2: Phenological observations for Leaves

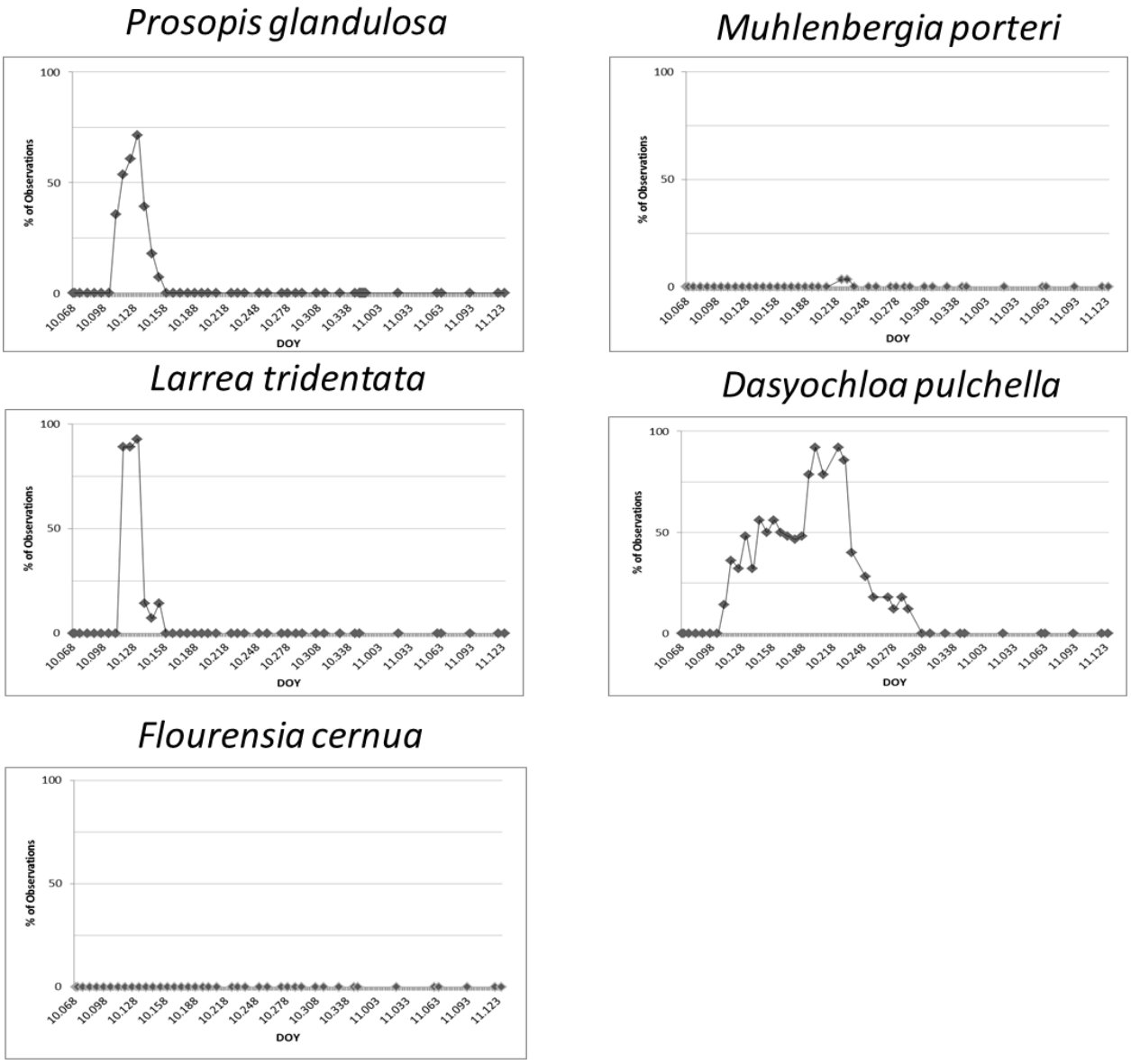

Figure 4.3: Phenological observations for Flower buds

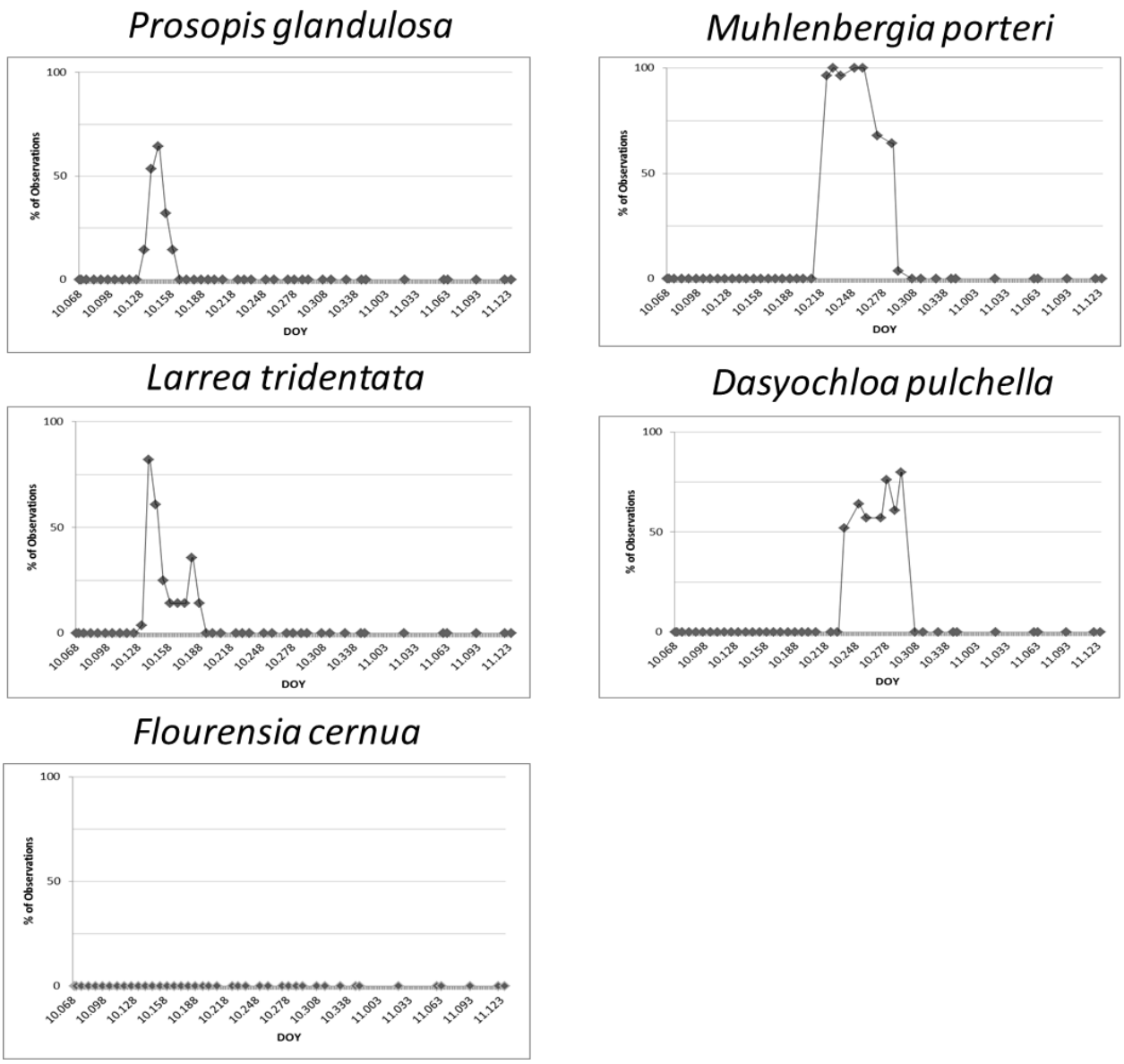

Figure 4.4: Phenological observations for Open flowers

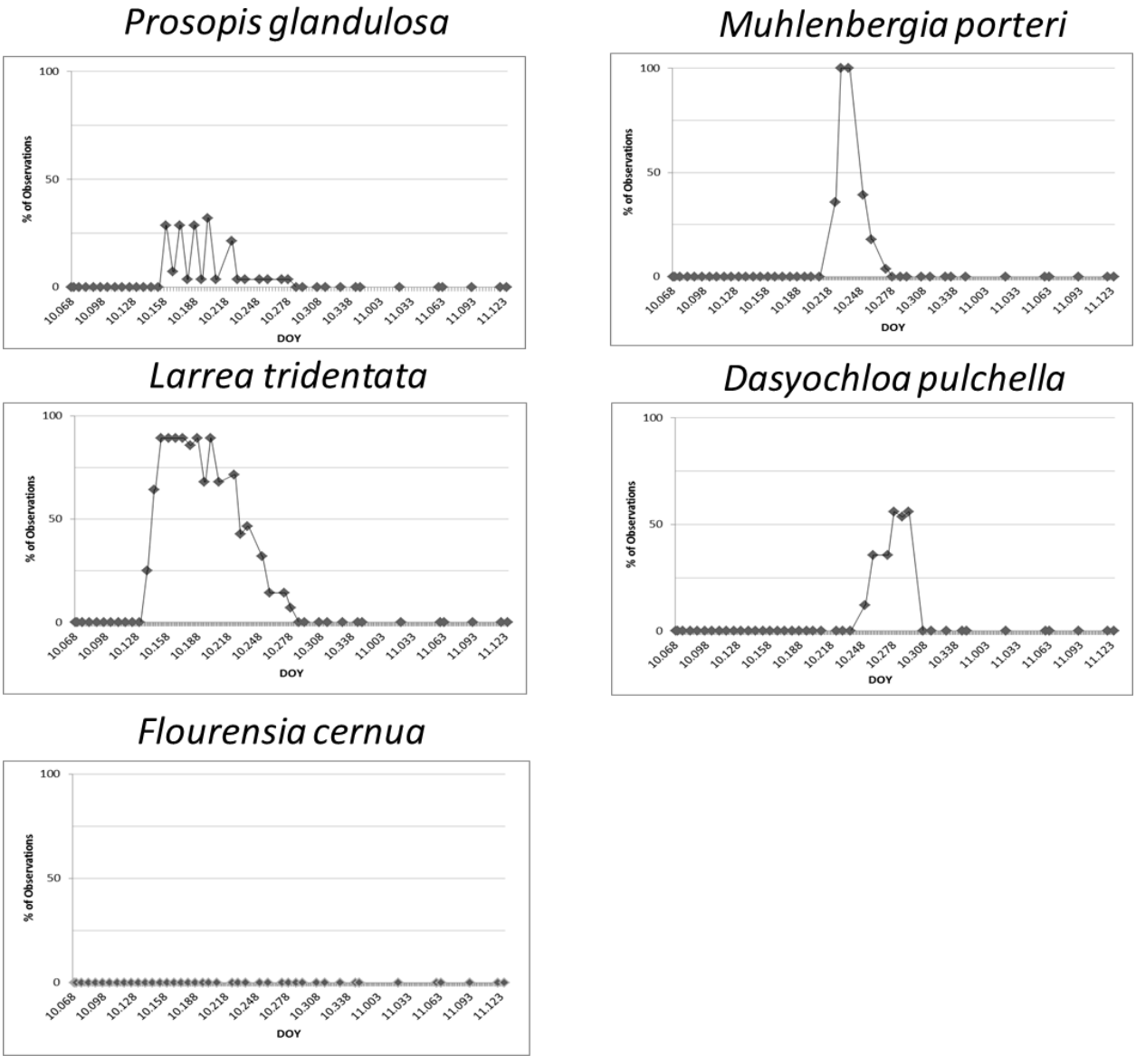

Figure 4.5: Phenological Observations for Fruits

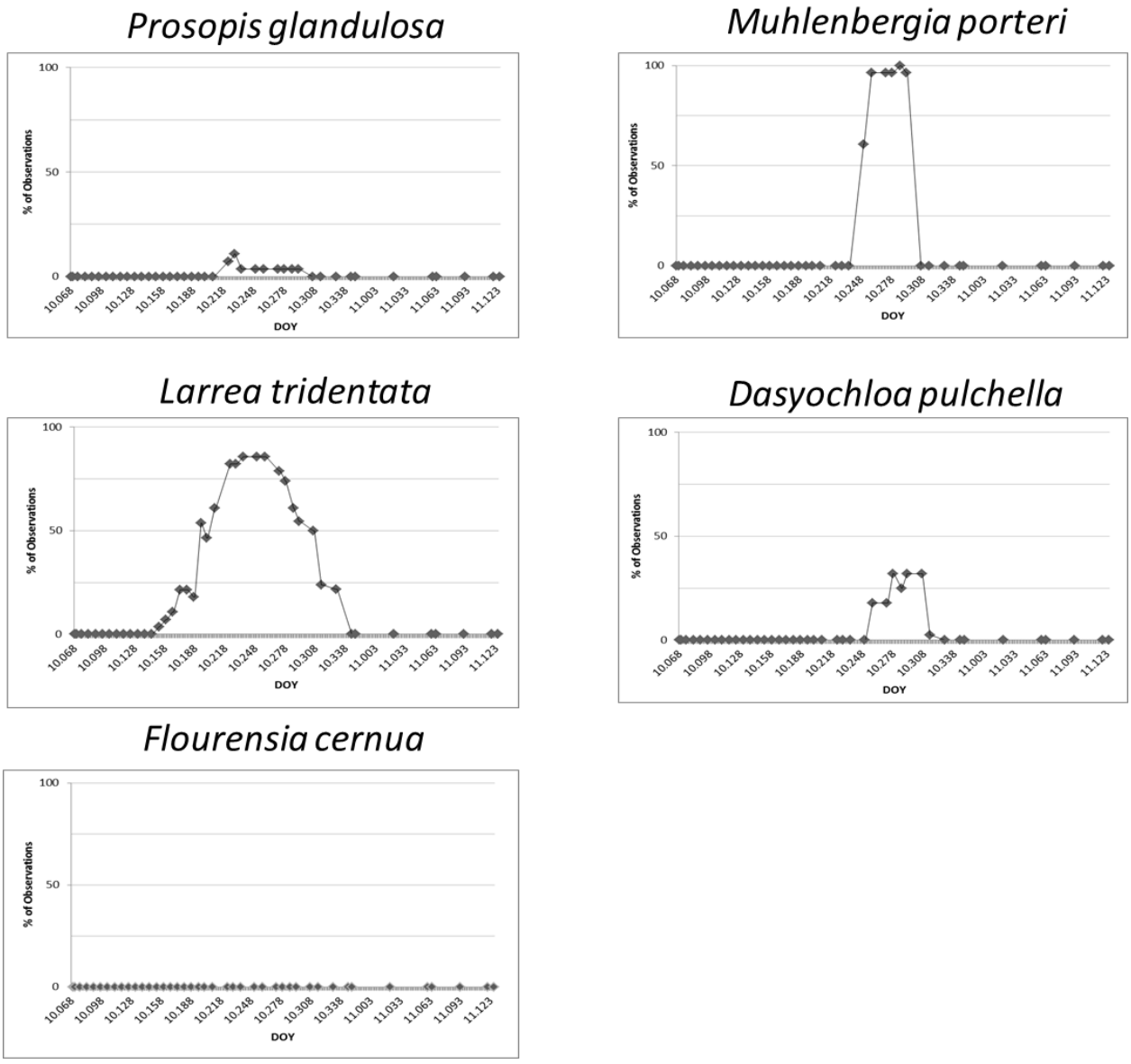

Figure 4.6: Phenological observations for Ripe fruits

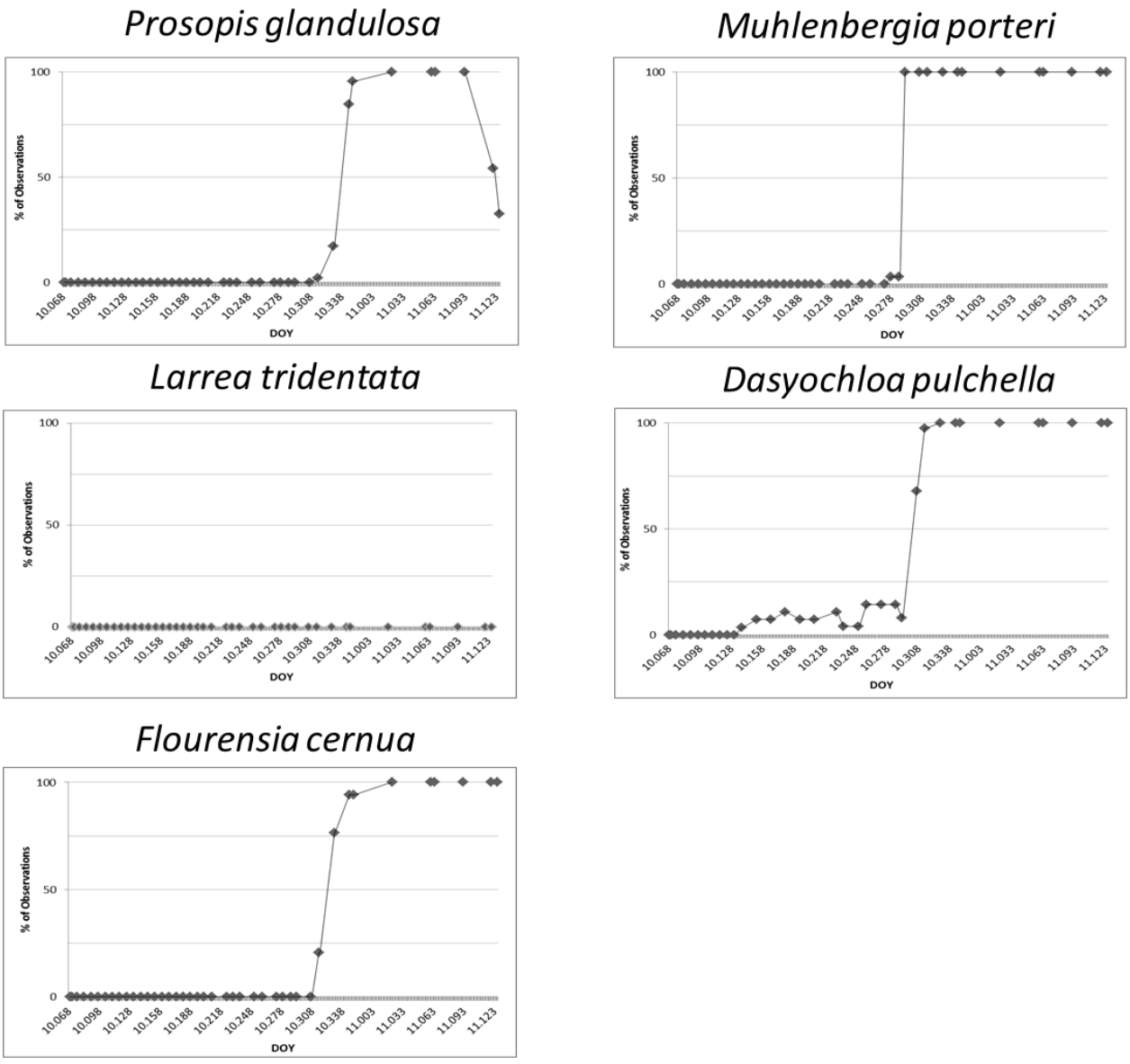

Figure 4.7: Phenological observations for All Leaves fallen/ withered

4.2. CLIMATE DATA

In this study, meteorological measurements were derived from an Eddy covariance tower. This included air temperature, relative humidity, wind speed and PAR as well as rainfall from 2010 and up to day 302 of 2011. The amount of cumulative precipitation was calculated and cross calibrated with phenological observations of focal plant species which dominate JER. Average annual precipitation for the Jornada Basin (1915 to 1995) is 245.1 mm (Havstad et al., 2006). The highest daily rainfall for year 2010 occurred on day 179 with 53.59 mm. Maximum daily precipitation reported for year 2011 was on day 223 with 18.54 mm. 2010 had more days with precipitation with 32 days of rain, compared to 2011 that had 30 rain days. Cumulative precipitation in 2011 was almost half that documented for 2010 (Fig. 4.8).

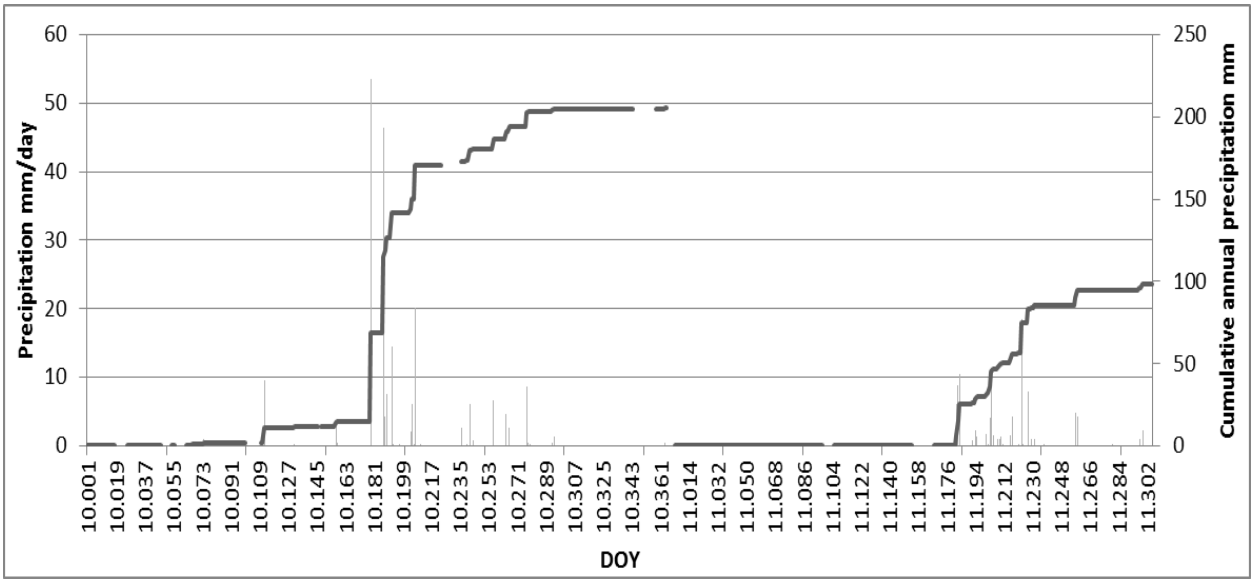

Figure 4.8 Annual precipitation for years 2010 and 2011

In this study air temperature, relative humidity, wind speed and photosynthetic active radiation (PAR) measurements were examined. The maximum air temperature recorded for year 2010 was on day 157 at 39.42°C, the lowest air temperature reported for 2010 was day 330 at -9.85°C. For 2011 day 178 had the maximum temperature reported with 39.29°C and the lowest temperature

was recorded on day 34 at -24.68°C. The relative humidity is given for both years studied in Figure 4.10. With a greater number of rain days and higher cumulative precipitation, 2010 was also more humid more often than 2011. Wind speed is given for both study years studied in Figure 4.11. For both years, wind speeds were highest in the spring and in the late afternoon. Maximum wind speed was recorded on day 364 of 2010 at 16.78 m/s, and in 2011 day 66 had the maximum wind speed reported at 15.82 m/s. Photosynthetic active radiation (PAR) is given for both years studied in Figure 4.12. Maximum photosynthetic active radiation reported for 2010 was on day 210 with 3287.24 m^2/s. In 2011, day 185 had the maximum (PAR) reported at 2919.66 m^2/s.

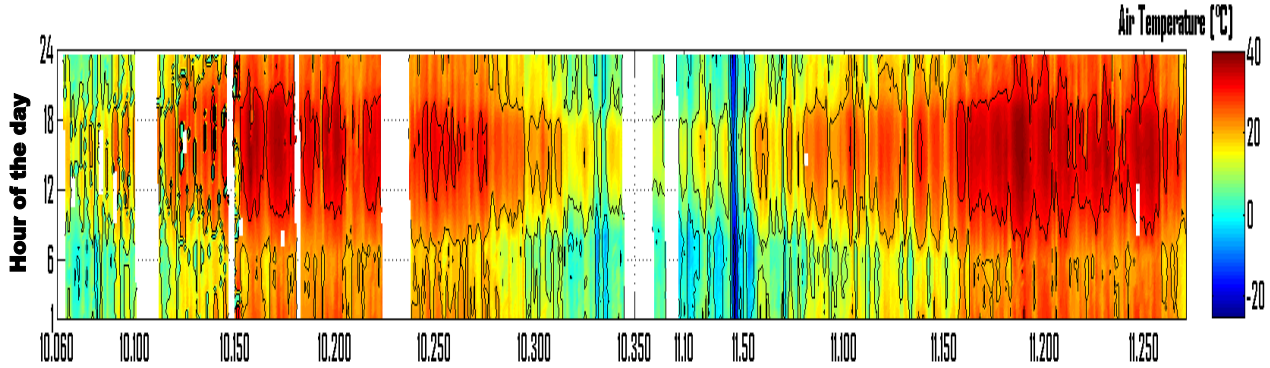

Figure 4.9: Air Temperature.

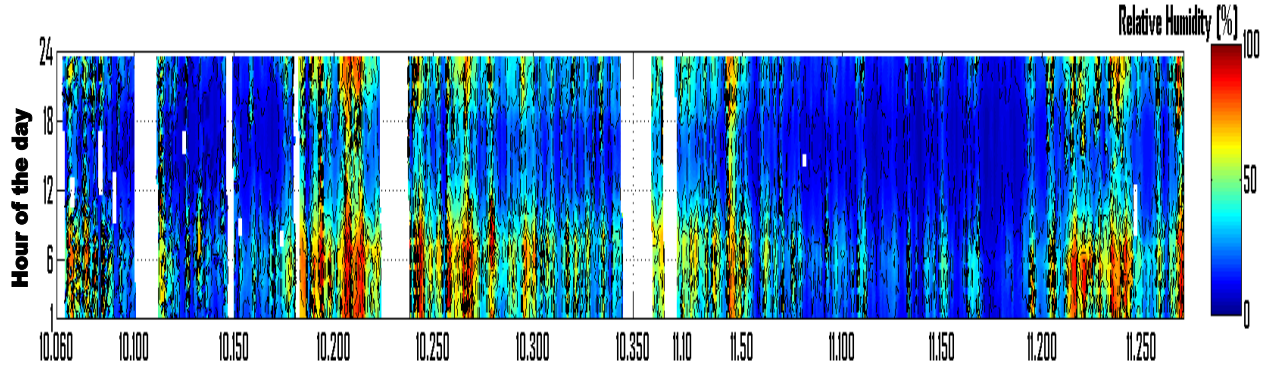

Figure 4.10: Relative Humidity

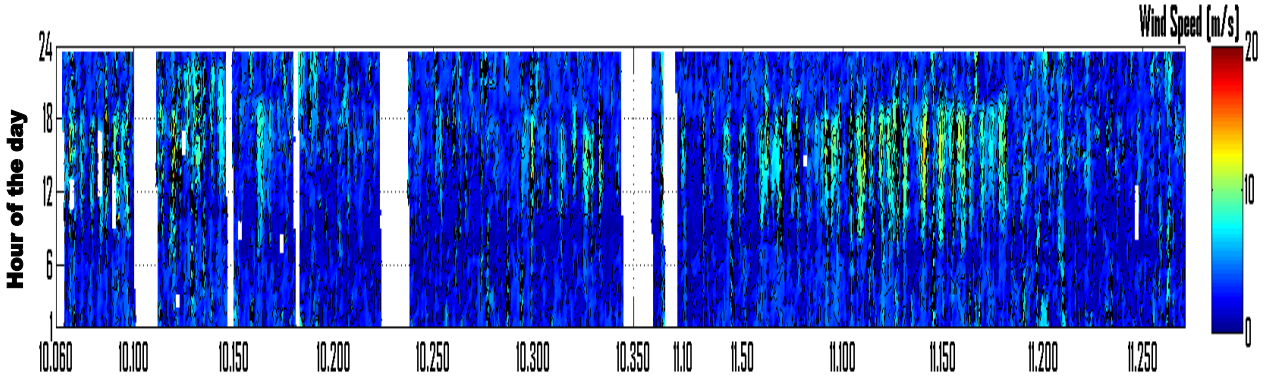

Figure 4.11: Wind Speed

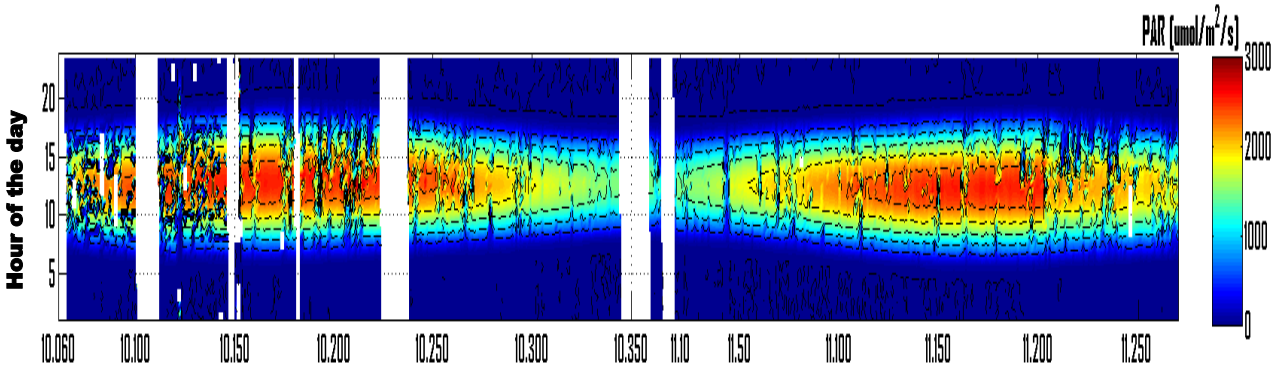

Figure 4.12: Photosynthetic active radiation (PAR)

4.3. WEBCAMS

A total of 456 days of webcam imagery were used to characterize landscape level phenology at the study site. Data used for this study were initiated on May 26, 2010 (day 146) and ended on August, 23, 2011 (day 235) and a total of 1,031 images were taken hourly between 7:00 to 19:00 each day. Several gaps exist in data collection due to technical problems that ranged from human error to technical failure as a result of extreme meteorological events such as the February 2011 freeze event. Image analyses were run on for ROIs that spanned 180 to 500 meters out from the flux tower for the three cameras (2, 3 and 4) viewing the flux tower footprint and the tramline footprint area for the remaining camera (camera 1). Images from each of the cameras on the same days of the year for 2010 and 2011 are given in Figure 4.13. Images that were analyzed were chosen manually by selecting images with the best possible quality around solar noon when light was most abundant shadows in the canopy were minimal. Images from excessively cloudy or rainy days were not used.

The three cameras (cameras 2, 3, 4) measuring the landscape phenology of the flux tower footprint had similar values and trends in the relative channel brightness and greenness indices measured (Fig. 4.15 and Fig. 4.14 A). The camera facing the tramline (camera 1) from which brightness and greenness values were derived demonstrated different channel brightness values and greenness indices to the cameras facing the flux tower footprint. Differences in the seasonal magnitude of the greenness indices (Fig. 4.14 A) were greater than that for total channel brightness (Fig. 4.14 B). Peak greenness in 2010 was observed on day 197 and the lowest greenness indices were recorded on day 141 of 2011. Greenness was greater in 2010 than for the same day of the year in 2011 (see Fig. 4.13). Differences between summer and winter greenness was also greater for the flux tower footprint than the tramline footprint (Fig. 4.14).

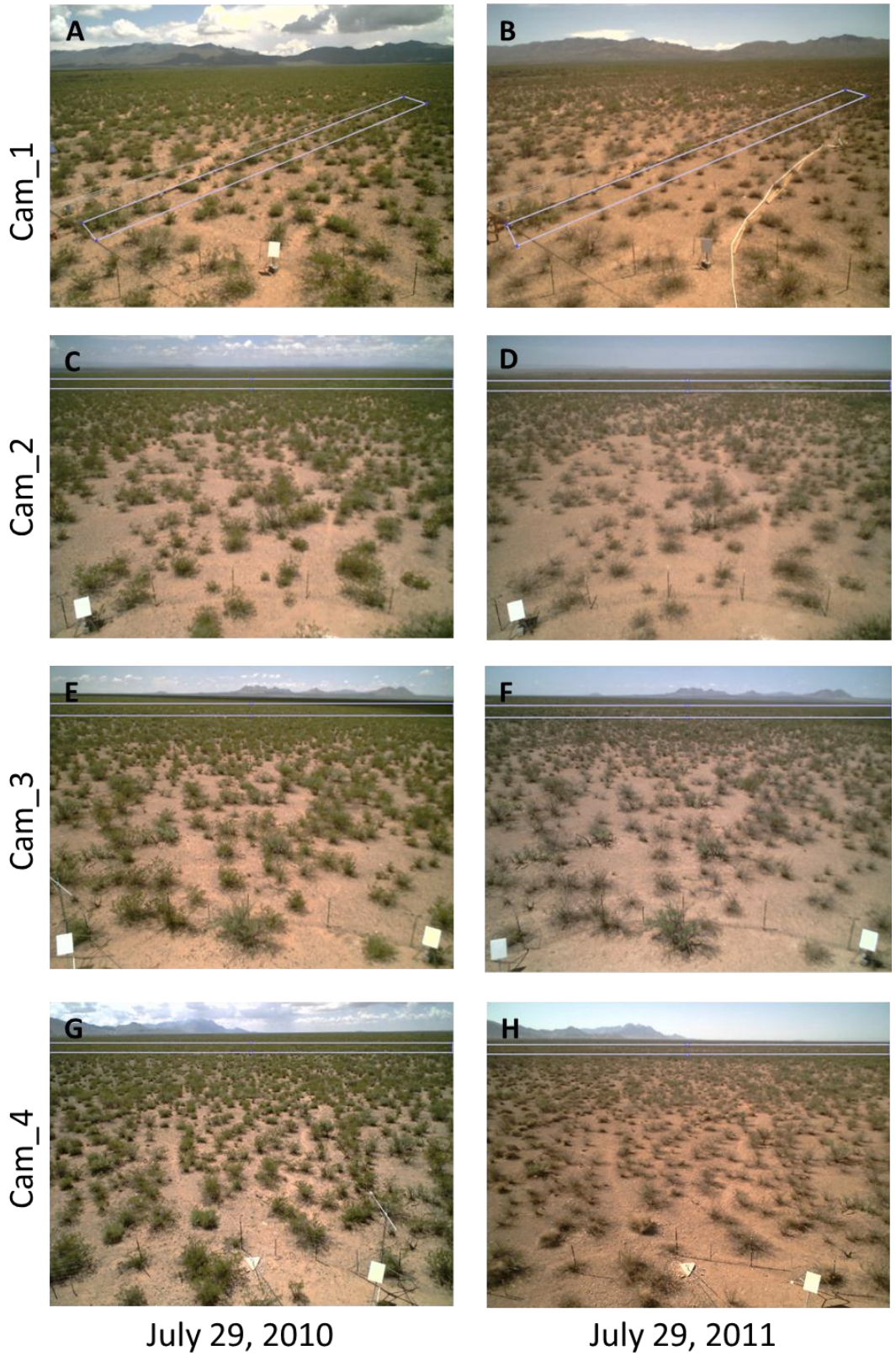

Figure 4.13: Comparison between year 2010 and 2011 (DOY 210) for the 4 cameras. The ROI used for digital image analysis is outlined in each camera image.

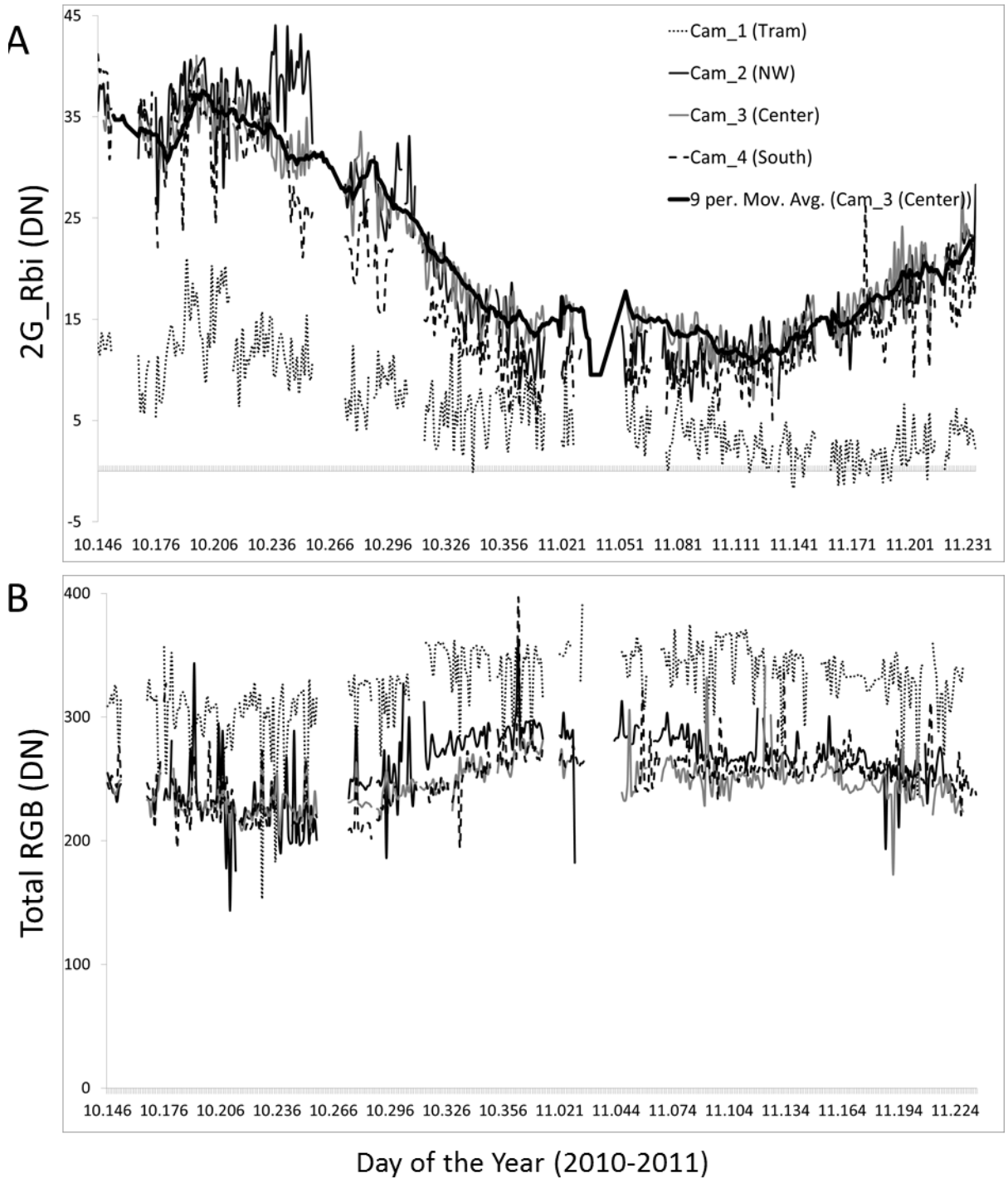

Figure 4.14: **A.** The green index calculated from channel brightness values (2G_RBi)= 2 x (green DN) – (red DN + blue DN). Plots reflected day-to–day variation in overall and relative channel brightness covering seasonal patterns such as autumn senescence, which occurred approximately on day 236 of 2010, when percent greenness started to decline. **B**. Total red green blue (RGB) DN= red DN + blue DN + green DN.

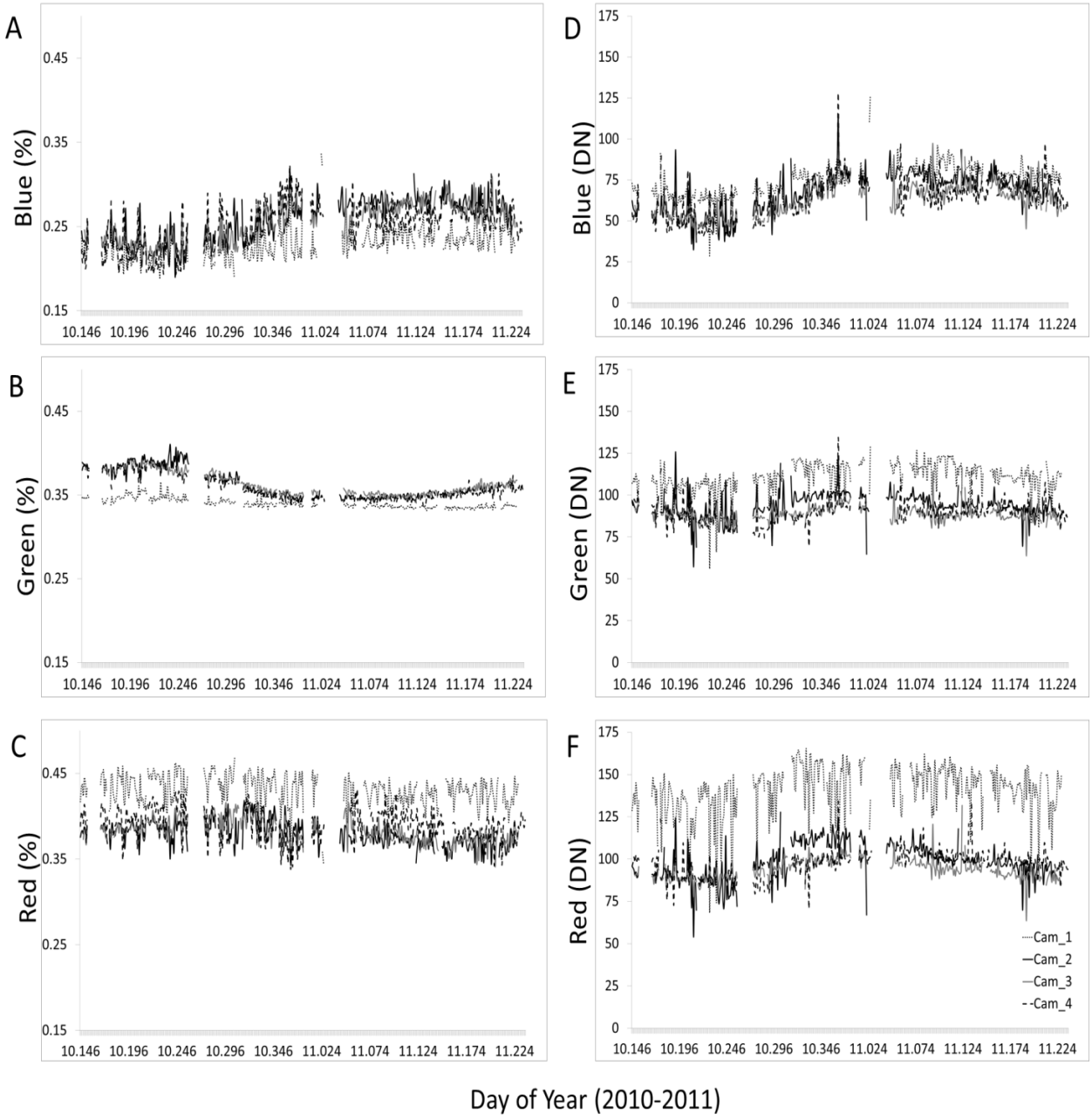

Figure 4.15: Time series of normalized webcam channel brightness values (i.e., channel % = channel DN/ total RGB DN) for the previously described regions of interest in the images from Jornada Basin Experimental Range Flux tower webcam. **A**. Blue %, **B**. green %, and **C**. red %. Time series of channel brightness values (digital number; DN) for the selected regions of interest at Jornada Basin Experimental Range flux tower webcams., **D**. blue DN, **E.** green DN**, F**. red DN

4.4. ROBOTIC TRAM MEASUREMENTS & CROSS CALIBRATION OF MEASUREMENTS

In this section of the study, seasonal species specific measurements from the same model of webcam used for phenocam measurements on the eddy tower were compared to NDVI-greenness derived from hyperspectral measurements collected with the robotic tram system (Fig. 4.16). NDVI and the Green Index responded in a similar manner for *P. glandulosa.* Both increased on approximately day 131 in 2010 and remained high until approximately day 306 of 2010. This was followed by an abrupt decline and stabilization from day 335 of 2010 through the end of the study period on day 119 of 2011. For *P. glandulosa* both indices are strongly correlated (R^2=0.8544, P <0.0001). For *L. tridentata,* NDVI fluctuated gently from day 110 of 2010 to day 223 of 2010, which was followed by a slight decrease from day 229 of 2010 that extended to day 119 of 2011. Compared to NDVI documented for *P. glandulosa*, *L. tridentata* was lower but seasonally more consistent. For *L. tridentata* both indices were well correlated (R^2=0.5805, P <.0001).

NDVI for *M. porteri* had light fluctuations from day 103 of 2010 to day 194 of 2010 followed by a gradual decline from day 208 of 2010 that extended through day 119 of 2011. The Green Index behaved differently, and green index had a dramatic increase on day 173 of 2010 that was extended through day 236 of 2010 followed by a gradual decline and stabilization from day 348 through the end of the study on day 119 of 2011. For *M. porteri* correlations were not well correlated (R^2=0.2046, P =0.0014). NDVI for *D. pulchella* fluctuated from day 103 of 2010 to day 187 of 2010 and gradually declined from day 194 of 2010 extending through the end of the study on day 119 of 2011. The green index for *D. pulchella* undulated throughout the study. For *D. pulchella,* there was a poor correlation between the greenness index and NDVI (R^2=-0.0162, P =0.551). For bare ground, NDVI fluctuated slightly from day 103 of 2010 to day 194 of 2010 and stabilized from day 201 of 2010 throughout the end of the study day 119 of 2011. The green index

for bare ground remained constant from day 103 of 2010 to day 306 of 2010 increasing slightly on day 335 throughout the end of the study day 119 of 2010. The correlation between NDVI and the greenness index for bare ground was poor (R^2=0.007814, P =0.2601). NDVI for all data (i.e. all species and bare ground) show a slight and minimal increase from day 103 of 2010 to day 236 of 2010 followed by a steady decline from day 250 of 2010 through the end of the study period on 119 of 2011. The green index for all data remained constant from day 103 of 2010 to day 180 of 2010 showing a slight increase on day 187 through day 229 of 2010 followed by a gently decline from day 250 of 2010 until the end of the study on day 119 of 2010. For all data, correlations between indices were low but significant (R^2=0.3773, P <0.0001).

Table 4.1: Results from linear regression performed between ecosystem-level greenness lg $2G - (Red + Blue)$ and NDVI (R800 – R680)/ R800 + R680). derived from hyperspectral measurements collected with the robotic tram system.

	R-square	*P*	*N*
Prosopis glandulosa	0.8544	<.0001	42
Larrea tridentata	0.5805	<.0001	39
Muhlenbergia porteri	0.2046	0.0014	43
Dasyochloa pulchella	-0.0162	0.551	41
Bare ground	0.00781	0.2601	40
All species	0.3773	<.0001	205

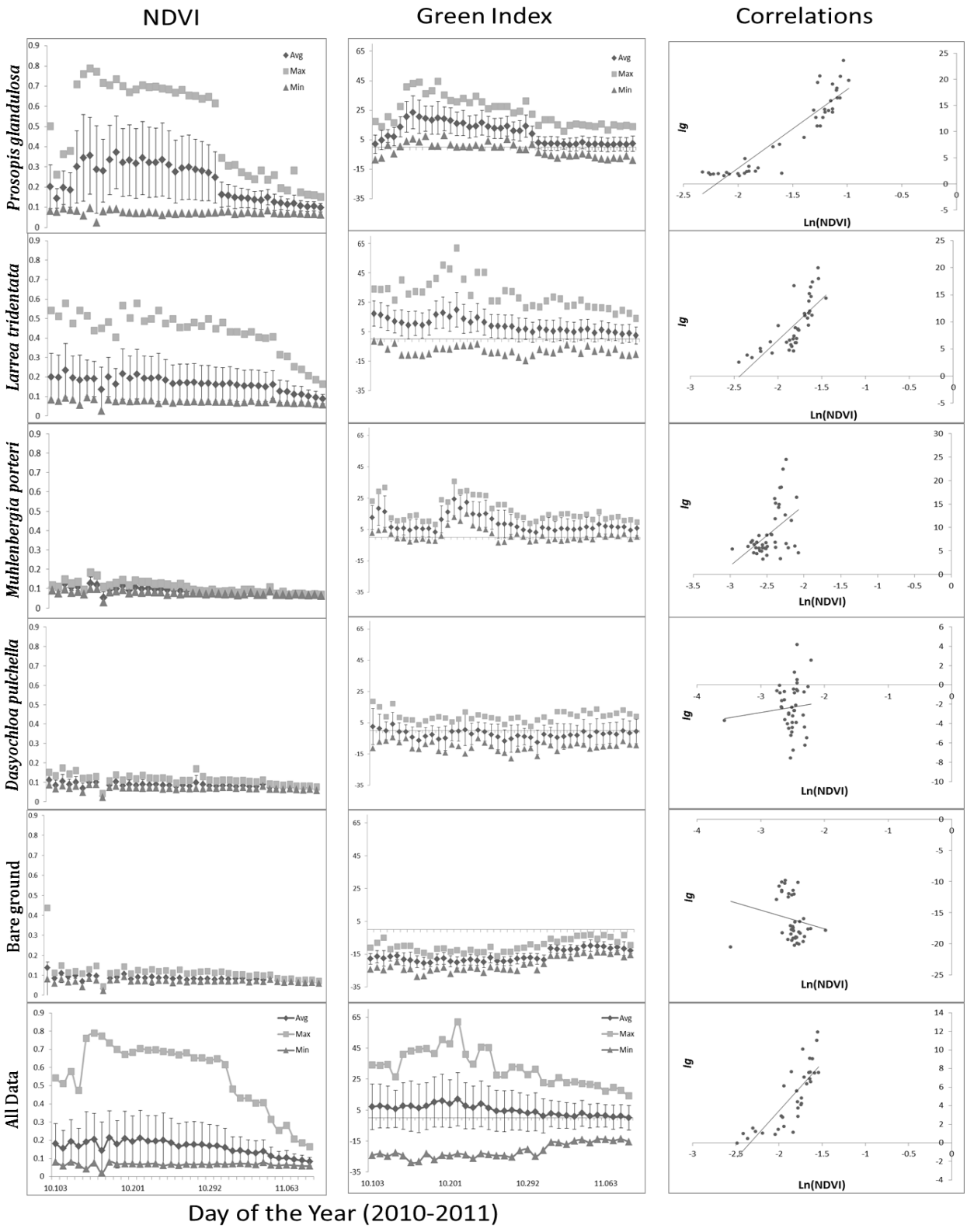

Figure 4.16: NDVI derived from hyperspectral reflectance measurements and Green Index derived from the Vx7000 webcam for the same ROIs along the tramline. A. *Prosopis glandulosa* B. *Larrea tridentata* C*. Muhlenbergia porteri*, D. *Dasyochloa pulchella*, E. Bare ground F. All data i.e. all species and bare ground. Note that there is no tarbush represented along the tramline.

5. Discussion and Conclusion

5.1. OBJECTIVE 1

The aim of objective 1 was to monitor the phenophase development of key plant species and the seasonal changes in physical environment to determine the following:

a. Do temporal patterns of phenological development differ between key plant species?

Phenological observations have been a focal area for scientific study for a long period of time (Bradley et al., 1999; Richardson et al., 2007). Due increased interest in climate change, scientific, economic and social consciousness, and need for understanding future ecosystem states, the importance and prevalence of phenological research has increased over the past few decades. Because plant phenology is strongly dependent on climate over weekly to decadal time scales, long-term phenological observations offer one of the best tools for understanding how climate change is impacting biota. This study supports such findings as the phenological patterns of the five focal plant species studied showed strong seasonal and phenological differences between species and within a species between the seasonally overlapping two years of study. This suggests that the phenology of the different species studied, is controlled by different environmental factors, and that climate appears to strongly influence these patterns.

b. How is plant phenophase development related to changes in the physical environment?

Using data on temporal and spatial variability in phenology, it is possible to estimate each species overall response to air temperature, precipitation, relative humidity, wind speed and photosynthetic active radiation (PAR). Studies of long-term changes in phenology have reported advancement in spring phenology as a result of winter warming (Fitter, 2002; Menzel et al., 2006). A long-term dataset (52 years) of Japanese plant phenological events in spring and autumn

(Ibañez et al., 2010) reported that for each degree Celsius increase in temperature, spring phenological events occurred up to 8 days earlier on average, and autumn phenological events occurred up to 4-5 days later. The data set presented in this study is short relative to the observation period needed to make such assessments. However, the overlapping late spring period of observation showed the phenology of most species in second year of study (2011) was particularly different from the same period in 2010. These differences are likely to be related to several climatic phenomenon over this time period.

On February 1st, 2011 an intense arctic air mass moved into southern New Mexico (Hardiman, 2011) and brought locally heavy snowfall followed by several days of extremely cold temperature. This was one of the coldest freeze events experienced in the region over the meteorological period of record in the El Paso – Las Cruces region. At the study site, the lowest temperature reported was on February 3rd (Day 34) when temperature dipped to a low of -24.68°C (Fig. 4.9). Furthermore year 2011 had a markedly lower cumulative precipitation than year 2010 (Fig. 4.8). *Larrea tridentata,* the only species with live leaves at the time of the freeze event was extremely responsive and breaking leaf buds died on 74% of the individuals studied. The other species studied were phenologically dormant when this event occurred. However, the spring phenological events for these species were delayed by at least several weeks compared to observations made at the same time in 2010. Thus, although this study cannot deterministically link phenological development with precise changes in climate variability and climate change trends due to the short term nature of the study, it does show that some of the dominant plant species present in a northern Chihuahuan Desert creosote shrubland are sensitive to climatic variability and possibly extreme climatic events. This suggests that they could be, therefore, excellent indicators of how climate variability and change could impact biota in the region.

5.2. OBJECTIVE 2

The aim of objective 2 was to develop a network of webcams and image processing software to automate the acquisition and post-processing of imagery suitable for documenting landscape-level phenological change by answering the following:

a. What type of camera is best suited to detecting phenological development through the extraction of Red Green and Blue (RGB) color bands?

Selecting a low-cost digital webcam that was able to detect phenological development through the extraction of (RGB) color bands was a challenge. Out of the vast range of possible cameras suited to conduct this study, four were selected for in-depth testing (Fig. 3.8). The following criteria were used for camera selection: Picture quality (megapixels), cost, and spectral quality. The Microsoft Vx 7000 was selected because it was the only camera system tested that met all three criteria. Testing of multiple cameras of this model also showed minimal spectral variability between cameras, further reinforcing the choice of this camera as an optimal choice for the study area.

Digital cameras have proven to be a cost efficient and effective way to monitor landscape phenology (e.g., Paruelo et al., 2000; Przeszlowska et al., 2006; Vanamburg et al., 2006; Richardson et al., 2007; Ahrends et al., 2008; Campillo et al., 2008; Crimmins and Crimmins, 2008; Kurc and Benton, 2010). However, in the reviewed literature we found different approaches to select the best suited cameras for this type of study. Surveillance cameras were used by (Richardson et al., 2007, 2009), professional digital cameras were deployed by (Crimmins and Crimmins, 2008), and game cameras were selected by (Kurc and Benton, 2010) for example. This was one of the first studies to test and implement a network of phenocams using webcams.

Compared to other studies (Richardson et al. 2007, 2009; Crimmins and Crimmins, 2008; Kurc and Benton, 2010) the approach used in this research was inexpensive related to other applications used in published literature. The system implemented at the JER cost approximately $255 (digital web-cams, $45 each (total $180); customized weatherproof housing, $10 each (total $40); Belkin USB Plus 4-Port Hub, $13; 36ft Tripp Lite U042-036 USB2.0 A/B repeater cable extension, $22), not including the PC required for image capture. Compared to the dual-detector spectrometer used in this research which costs approximately $20,000 the webcam network is extremely inexpensive, although it does not present the spectral resolution captured by the spectrometer. For extensive sensor deployments measuring the phenology of individual plants or landscapes, webcams present a cost effective choice.

b. Can software be developed to automate the process of digital image acquisition, storage, and analysis?

This study provides evidence that it is possible to develop software to automate digital image capture and processing for a network of phenocams at the JER study site. The software designed and implemented as a component of this study consists of a set of Matlab programs to facilitate image acquisition, storage and analysis. The analytical software suite includes a set of tools to aid image viewing that is useful for quality control, selection of different regions of interest, and image analysis and visualization of greenness indices. This component of the study benefited from interdisciplinary cooperation between Computer Science and Environmental Science students through UTEP's Cyber-ShARE Center of Excellence.

5.3. OBJECTIVE 3

The aim of objective 3 was to cross-correlate measurements of landscape-level phenological development using webcams with indices of plant productivity derived from hyperspectral reflectance measurements collected with a robotic tram system. This activity specifically addressed the following questions:

a. Do the optical properties captured by webcams correlate with the dynamics of plant phenology?

Landscape-level phenology trends derived from a robotic tram system were cross correlate with image-derived greenness from a network of digital webcams mounted on the eddy covariance tower. The results from the study spanned May 2010 to August 2011 and demonstrate that imagery from digital webcams were able to detect landscape-level phenological development using greenness indices calculated by the software discussed above that used the RGB color bands of the digital webcams. Generally, greening trends documented with the webcams matched the occurrence of green leaves and breaking leaf buds of key plant species documented in the phenophase study outlined above. Trends mostly closely matched the phenophase development of creosote and mesquite, which make up the majority of biomass at the site. Trends in landscape greening trends also documented the delay in greenup documented between 2010 and 2011 in the phenophase study above, potentially related to extreme climatic events in early 2011.

Tracking phenology using digital webcam imagery has a number of advantages over field observations (Richardson et al., 2007). Old-style plant phenological monitoring relies on an observer which can be imprecise, somewhat objective, and expensive. Findings in this study show that it is possible to document landscape level phenology with a relatively inexpensive webcam network, which can capture numerous images per day and be automatically analyzed with the

newly developed software described above. This study also provides evidence that utilizing novel technologies such as near-remote sensing instruments can save time, energy, money and effort to make phenological observations in the Northern Chihuahuan Desert.

b. Do the optical properties captured by webcams capture the spatial and temporal variability of plant productivity indices derived from hyperspectral reflectance measurements?

Digital imagery was analyzed to detect phenological patterns of a Northern Chihuahuan Desert evergreen shrub canopy as described above. These trends were compared with estimates of canopy-scale biomass (NDVI) derived from a robotic tram system upon which hyperspectral reflectance was measured weekly with a Unispec spectrometer (UniSpec DC, PP Systems Inc., Amesbury MA, USA). Like other studies (Gamon et al., 2006) that have utilized a robotic tram system to document the landscape phenology, this study also showed success with this system. Moreover, the study showed that greenness indices derived from the webcams matched those derived from hyperspectral reflectance for most species.

In this study seasonal NDVI from 110 plots were correlated with digital image-derived greenness. Strong correlations were observed for *P. glandulosa* (Fig. 4.16 A) and *L. tridentata* (Fig. 4.16 B), which have the greatest biomass and cover compared to other species at the site. For species such as *M. porteri* (Fig. 4.16 C), *D. pulchella* (Fig. 4.16D) and for bare ground (Fig. 4.16 E) patterns were not well correlated between the two optical sampling methods. This could be attributed to differences in structure and the cover of green biomass, which differed between these species.

This study demonstrated a good cross-correlation between landscape-level phenological development using webcams and spectral indices derived from a robotic tram system.

Hyperspectral spectroradiometers are expensive, and are therefore limiting in extensive automated sampling programs (Garrity et al., 2010). However, the monitoring effort demonstrated with the inexpensive webcams shows that similar trends can be derived and could provide an alternate solution for extensive sampling in similar ecosystems.

5.4. CONCLUSIONS

The overarching aim of this study was to develop a low-cost network of webcams that were able to monitor the phenological canopy development of a Chihuahuan desert shrubland, including capture of the spatial and temporal variability associated with seasonal and interannual plant productivity. With collaborations through UTEP's Cyber-ShARE Center and interdisciplinary collaboration between computer science and environmental science development and testing of such a system was accomplished. The phenophase monitoring, network of phenocams and phenological observations associated with the robotic tram system remain active. Given longer term phenological time series, the controls of seasonal and interannual variability in phenology will be possible using the protocols, inexpensive webcam network, and analytical software developed in this study.

5.5. SUGGESTIONS FOR FUTURE WORK

To improve current understanding of how phenological development will change in response to a changing environment, an extensive data set is required. The cyberinfrastructure located at JER creates an extraordinary benchmark to capture the data needed for such advancement of knowledge such as digital imagery, meteorological data, hyperspectral measurements and field-based phenological observations. Digital image-derived greenness indices are likely to not only be

important to quantifying landscape scale phenology, but also estimating landscape scale carbon uptake and how plant biomass controls energy production supporting trophic interactions.

Image-derived greenness can also have the potential of being related to remotely sensed depictions of land surface phenology using a number of remote sensing platforms such as unmanned aerial vehicles, moderate spatial resolution Landsat, and coarse spatial resolution MODIS imagery to track the onset and dynamics of landscape phenology and productivity. Such an activity is likely to provide plant and landscape level understanding of processes driving regional scale phenological dynamics. All of these applications are likely to benefit greatly from novel cyberinfrastructure development, which can not only improve data processing efficiency as in this study, but also facilitate data sharing with the greater research community.

6. References

1. Ahl, D. E., Gowers, S. T., Burrows, S. N., Shabanov, N. V., Myneni, R. B., Knyazikhin, Y., 2006. Monitoring spring canopy phenology of a deciduous broadleaf forest using MODIS. Remote sensing Environment 104: 88-95.
2. Ahrends, H.E., Brugger, R., Stockli, R., Schenk, J., Michna, P., Jeanneret, F., Wanner, H., Eugster, W., 2008. Quantitative phenological observations of a mixed beech forest in northern Switzerland with digital photography. Journal of Geophysical Research-Biogeosciences. 113: (G04004), doi: 10.1029/2007JG000650.
3. Aitken, Y., 1974. Flowering time, climate and genotype: the adaptation of agricultural species to climate through flowering responses. Melbourne University Press, Melbourne.
4. Allred, K. W., 1996. Vegetative changes in New Mexico rangeland. New Mexico Journal of Science 36: 168-229.
5. Anderson, J., Peters, D. C., Rango, D. C., Steele, C., 2007. Linking ground observations, simulation model output, and remote sensing data to characterize phenology across diverse arid landscapes. American Society of Photogrammetry and Remote Sensing Meetings.
6. Ansley, R. J., Wu, B. X., Kramp, A., 2001. Observation: Long-term increases in mesquite canopy cover in a North Texas savanna. Journal Range Management. 54: 171-176.
7. Bachelet, D., Wodzell, S. M., Reynolds, J. F., 1988. Simulation model using environmental cues to predict phenomenologies of winter and summer annuals in the northern Chihuahuan Desert. Advances in Environmental Modeling.
8. Badeck, F. W., Bondeau, A., Bottcher, K., Doktor, D., Lucht, W., Schaber, J. et al., 2004. Responses of spring phenology to climate change. New Phytologist. 162: 295-309.
9. Bowers, J. E., Dimmitt, M. A., 1994. Flowering phenology of six woody plants in the northern Sonoran Desert. Bulletin of the Torrey Botanical Club. 121(3): 215-229.
10. Bradley, N. L., Leopold, A., Ross, C., Wellington, J. H., 1999. Phenological changes reflect climate change in Wisconsin. Ecology. 96: 9701-9704.
11. Browning, D. M., Laliberte A., Rango, A., Herrick, J. E., in progress. Prospects of phenological monitoring in an arid soutyhwestern U.S. rangeland using field observations with hyperspatial and moderate resolution imagery.
12. Campillo, C., Prieto, M. H., Daza, C., Monino, M. J., Garcia M. I., 2008. Using digital images to characterize canopy coverage and light interception in a processing tomato crop. Hortscience. 43(6): 1780-1786.
13. Cayan, D. R., Kammerdiener, S. A., Dettinger, M. D., Caprio, J. M., Peterson, D. H., 2001. Changes in the onset of spring in the western United States. Bulletin of the American Meteorological Society. 82:399-415.
14. Chew, R., 1982. Changes in herbaceous and suffrutescent perennials in grazed and ungrazed desertified grassland in southeastern Arizona, 1958-1978. The American Midland Naturalist. 108(1):159-169.
15. Clayton, W. D., Renvoize, S. A., 1986. Genera Graminum grasses of the world. Kew bulletin additional series XIII. Royal Botanical Gardens, Kew, London.
16. Crimmins, M. A., Crimmins, T. M., 2008. Monitoring plant phenology using digital repeat photography. Environmental Management. 41(6): 949-958.
17. De Soyza, A. G., Killingbeck, K. T., Whitford, W. G., 2004. Plant water relations and photosynthesis during and after drought in a Chihuahuan desert arroyo. Journal of Arid Environments. 59(1): 27-39.

18. Dick-Peddie, W. A., 1993. New Mexico vegetation: past, present, and future. Albuquerque, NM: University of New Mexico. Press. 244p.
19. Dokoozlian, N. K., 1999. Chilling Temperature and Duration Interact on the Bud break of "Perlette" Grapevine Cuttings. HortScience. 34(6).
20. Duisberg, P. C., Shires, L. B., Botkin, C. W., 1949. Determination of nordihydroguaiaretic acid in the leaf of Larrea divaricata (creosote bush). Analyt. Chem. 21:1393-1398.
21. Duncan, J., Stow, D., Franklin, J., Hope, A., 1993. Assessing the relationships between spectral vegetation indices and shrub cover in the Jornada Basin, New Mexico. International Journal Remote Sensing. 14 (18): 3395-3416.
22. Dunne, J. A., Harte, J., Taylor K. L., 2003. Subalpine meadow flowering phenology responses to climate change: integrating experimental and gradient methods. Ecological Monographs. 73: 69-86.
23. Dwight, R., Clark, M. S., 1975. Vegetation responses to grazing, rainfall, site condition, and mesquite control on semi-desert range. Res. Pap. RM-149. Fort Collins, Co: U.S. Department of agriculture, Forest Service, Rocky Mountain Forest and Range Experiment Station. 24(4887).
24. Estell, R. E., Frederickson, E. L., Anderson, D. M., Havstad, K. M., Remmenga, M. D., 1998. Relationship of tarbush leaf surface terpene profile with livestock herbivory. Journal of Chemical Ecology. 24: 1-12.
25. Felker, P., 1979. Mesquite: an all-purpose leguminous and land tree. In GA. Ritchie (ed.), New Agricultural crops, American association for the Advancement of Science, Westview Press, golden, CO. p. 89-132.
26. Fisher, C. E., Meadors, E. D., Robinson, P. T., Morton Marion and H. L., 1959. Control of mesquite on grazing lands. Texas Agr. Exp. Sta Bull. 935. P. 24.
27. Fitter, A. H., Fitter, R. S. R., 2002. Rapid changes in flower time in British plants. Science 296:1689-1691.
28. Forrest, J., Inouye, D. W., Thomson, J. D., 2010. Flowering phenology in subalpine meadows: Does climate variation influence community co-flowering patterns?. Ecology, p. 431-440.
29. Franco, A. C., de Soyza, A. G., Virginia, R. A., Reynolds, J. F., Whitford, W. G., 1994. Effects of plant size and water relations on gas-exchange and growth of the desert shrub Larrea tridentata. Oecologia. 97(2): 171-178.
30. Gamon, J. A., Rahman, A. F., Dungan, J. L., Schildhauer, M., Hummrich, K. F., 2006. Spectral Network (SpecNet)-What is it and why do we need it? Remote Sensing of Environment 103: 227-235.
31. Garrity, S. R., Vierling, L. A., Bickford, K., 2010. A simple filtered photodiode instrument for continuous measurements of narrowband NDVI and PRI over vegetated canopies. Agricultural and Forest Meteorology 150: 489-496.
32. Geesing, D., Felker, P., Bingham, R. L., 2000. Influence of mesquite (Prosopis glandulosa) on soil nitrogen and carbon development: Impications of global carbon sequestration. Journal of Arid Environments. 46: 157-180.
33. Gibbens, R. P., Beck, R. F., Mcneely, R. P., Here, C. H., 1992. Recent rates of mesquite establishment in the northern Chihuahuan Desert. Journal of Range Management. 45: 585-588.
34. Gibbens, R. P., Havstad, K. M., Billheimer, D. D., Herbel, C. H., 1993. Creosotebush vegetation after 50 years of lagomorph exclusion. Oecologia. 94:2010-217.
35. Gibbens, R. P., Lenz, J. M., 2001. Root systems of some Chihuahuan desert plants. Journal of Arid Environments. 49(2): 221-263. [78961]

36. Gile, L. H., Hawley, J. W., Grossman, R. B., 1981. Soils and Geomorphology in the Basin and Range Area of Southern New Mexico-Guidebook to the Desert Project. Memoir 36, NM Bureau of Mines and Minerals Resources, Socorro, NM.
37. Goswami, S., Gamon, J. A., Tweedie, C. E., 2011. Surface hydrology of an arctic ecosystem: Multiscale analysis of a flooding and draining experiment using spectral reflectance.
38. Haggerty, B. P., Mazer, S. J., 2008. The Phenology handbook; guide to phenological monitoring for students, teachers, families, and nature enthusiasts. UCSB Phenology Stewardship Program.
39. Hamerlynck, E. P., Mcauliffe, J. R., Smith, S. D., 2000. Effects of surface and sub-surface soil horizons on the seasonal performance of Larrea tridentata (Creosotebush). Functional Ecology (14): 596-606.
40. Hardiman, M., 2011. Intense cold Wave of February 2011, National Weather Service El Paso, TX/Santa Teresa, NM.
41. Harris, G. A., 1977. Root Phenology as a factor of completition among grass seedlings. Journal of Range Management. Vol. 30, No.3: 172-177.
42. Havstad, M. K., Huenneke, L. F., Schlesinger, W. H., 2006. Structure and function of a Chihuahuan Desert Ecosystem. Long-Term Ecological Research Network series. Oxford University Press.
43. Hochstrasser, T., Peter, D., Fehmi, J., VonFinger, K., 2002. A Bibliography of Important Plant species in the Chihuahuan Desert of North America (1904-2002). U.S. Army Corps of Engineers, Construction Engineering Research Laboratory. ERDC/CERL SR-02-8.
44. Hoffmann, J. H., Impson, F. A. C., Moran, V. C., 1993. Competitive Interactions between two Bruchid species (Algarobius spp.) introduced into South Africa for biological control of mesquite (Prosopis spp.). Biological control. 3: 215-220.
45. Huete, A. R., Didan, K., 2006. Amazon rainforest green-up with sunlight in dry season. Geophysical Research Letters 33(L06405), doi: 10.1029/2005GL025583.
46. Ibañez, I., Primack, R. B., Miller-Rushing, A. J., Ellwood, E., Higuchi, H., Don Lee, S., Kobori, H., Silander, J. A., 2010. Forecasting phenology under global warming. Philosophical Transactions. 365: 3247-3260.
47. Jenkins, J. P., Richardson, A. D., Braswell, B. H., Ollinger, S. V., Hollinger, D. Y., Smith, M. L., 2007. Refining light-use efficiency calculations for deciduous forest canopy using simultaneous tower-based carbon flux and radiometric measurements. Agricultural and Forest Meteorology. 143:64-79.
48. Joffre, R., Rambal, S., 1988. Soil water improvement by trees in rangelands in southern Spain. Acta Oecologia Plantarum. 9:40-42.
49. Jornada Basin LTER IV; Linkages in semi-arid landscapes. Jornada LTER-IV Consortium.
50. Justice, C. O., Townshend, J. R. G., Tucke C. J., 1985. Analysis of the phenology of global vegetation using meteorological satellite data. International Journal of Remote Sensing. 6:8, 1271-1318.
51. Kemp, P., 1983. Phenological patterns of Chihuahuan desert plants in relation to the timing of water availability. Journal of Ecology 71(2):427-436.
52. Kingsbury, J. M., 1964. Poisonous plants of the United States and Canada. Englewood Cliffs, NJ: Prentice-Hall. 626 p.
53. Kochmer, J. P., Handel, S. N., 1986. Constraints and competition in the evolution of flowering phenology. Ecology Monographs. 56(4): 303-325.

54. Kurc, S. A., Benton, L. M., 2010. Digital image-derived greenness links deep soil moisture to carbon uptake in creosotebush-dominated shrubland. Journal of Arid Environments. 74: 585-594.
55. Leith, H., 1976. Phenology and seasonality Modeling (Springer, New York), pp.369-401.
56. Livingston, M., Roundy, B. A., Smith, S. E., 1995. Association of native grasses and overstory species in southern Arizona. In: Roundy, B. A.; McArthur, E. D., Halley, J. S., Mann, D. K., compliers. Proceedings: wild land shrub and arid land restoration symposium. U.S. Department of agriculture, Forest Service, Intermountain Research Station: 202-208.
57. Loomis, R. S., Connor, D. J., 1992. Crop ecology: Productivity and management in agriculture systems. Cambridge University Press, New York.
58. Meinzer, F. C., Rundel, P. W., Sharifi, M. R., Nielsen, E. T., 1986. Turgor and osmotic relations of the desert shrub Larrea tridentata. Plant, Cell & Environment. 9: 467-475.
59. Menzel, A., Sparks, T. H., Estrella, N., Koch, E., Aasa, A., Ahas, R., Almkubler, K., Bissolli, P., 2006. European phenological response to climate change matches the warming pattern. Global Change Biology. 12 (10): 1969-1979.
60. Miller, R. E., Huenneke, L. F., 2000. The relationship between density and demographic variation within a population of Larrea tridentata. Southwestern Naturalist. 45 (3): 313-321.
61. Morisette, J. T., Richardson, A. D., Knapp, A. K., Fisher, J. I., Graham, E. A., Abatzoglou, J., 2009. Tracking the rhythm of the seasons in the face of global change: phenological research in the 21st century. Frontiers in Ecology and the Environment. 7: 253-260.
62. Neilson, R. P., 1993. Transient ecotone response to climatic change: some conceptual and modeling approaches. Ecological Application. 3:385-395.
63. Odening, W. R., Strain, B. R., Oechel, W. C., 1974. The effect of decreasing water potential on net CO2 exchange of intact desert shrubs. Ecology 55: 1086-1095.
64. Ogle, K., Reynolds, J. F., 2002. Desert dogma revisited: coupling stomatal conductance and photosynthesis in the desert shrub, Larrea tridentata. Plant Cell and Environment 25(7):909-921.
65. Parker, L. W., Fowler, H. G., Ettershank, G., Withford, W. G., 1982. The effects of subterranean termite removal on desert soil nitrogen and ephemeral flora. Journal of Arid Environments. 5: 53-59.
66. Parmesan, C., Yohe, G., 2003. A globally coherent fingerprint of climate change impacts across natural systems.Nature 421: 37-42.
67. Paruelo, J. M., Lauenroth, W. K., Roset, P. A., 2000. Technical note: estimating aboveground plant biomass using a photographic technique. Journal of Range Management. 53(2): 190-193.
68. Peinetti, H., R, Fredrickson, E. L., Peters, D., Cibils, F., Roacho-Estada, J. O., Laliberte, A. S., 2011. Foraging behavior of heritage versus recently introduced herbivores on desert landscapes of the American Southwest. Ecosphere 2: 5.
69. Peñuelas, J., Boada, M., 2003. A global change-induced biome shift in the Montseny Mountains (NE Spain). Global Change Biology. 9:131-140.
70. Peñuelas, J., Filella, I., Zhang, X. Y., Llorens, L., Orgaya, R., Lloret, F., Comas, P., Estiarte, M., Terradas, J., 2004. Complex spatiotemporal phenological shifts as a response to rainfall changes. New Phytol. 161(3):837-846.
71. Peters D. P., 2002. Recruitment potential of two perennial grasses with different growth forms at a semiarid-arid transition zone. American Journal of Botany. 89: 1616-1623.

72. Pezzani, F., Montaña, C., Guevara, R., 2006. Associations between arbuscular mycorrhizal fungi and grasses in the successional context of a two-phase mosaic in the Chihuahuan Desert. Mycorrhiza. 16: 285-295.
73. Powell, A., M., 1988. Trees and shrubs of Trans-Pecos Texas: Including Big Bend and Guadalupe Mountains National Parks. Big Bend National Park, TX: Big Bend Natural History Association. 536:6130.
74. Powell, A. M., 2000. Grasses of the Trans-Pecos and Adjacent areas. Iron Mountain press.
75. Przeszlowska, A., Trlica, M. J., Weltz, M. A., 2006. Near-ground remote sensing of green area index on the shortgrass pairie. Rangeland Ecology and Management. 59(4): 422-430.
76. Rathcke, B. J., 1983. Competition and facilitation among plants for pollination. Pollination biology. Academic press, New York, New York, USA. 305-329.
77. Rathcke, B. J., Lacey, E. P., 1985. Phenological patterns of terrestrial plants. Annual Review of Ecology and Systematics. 16:179-214.
78. Reynolds, J. F., 1986. Adaptive strategies of desert shrubs with special reference to the Creosotebush (*Larrea tridentata* [DC] Cov.). In Patterns and process in desert ecosystems. Editor W. G. Whitford, Pattern and Process in Desert Ecosystems, University of Mexico Press, Albuquerque, pp. 19-49.
79. Richardson, A. D. Jenkins, J. P., Braswell, B. H., Hollinger, D. Y., Ollinger, S. V., Smith, M. L., 2007. Use of digital webcam images to track spring green-up in a deciduous broadleaf forest. Oecologia. 152(2):323-334.
80. Richardson, A. D., Braswell, B., Hollinger, D. Y., Jenkins, J. P., Ollinger, S. V., 2009. Near-surface remote sensing of spatial and temporal variation in canopy phenology. Ecological Society of America. 19(6): 1417-1428.
81. Root, T. L., Price, J. T., Hall, K. R., Schneider, S. H., Rosenzweig, C., Pounds, J. A., 2003. Fingerprints of global warming on wild animals and plants. Nature. 421: 57-60.
82. Robertson, C., 1985. The philosophy of flower seasons and the phenological relations of the entomophilous flora and the anthophilous insect fauna. American Naturalist. 29: 97-117.
83. Rosenzweig, C., Casassa, G., Karoly, D. J., Imeson, A., Liu, C., Menzel, A., Rawlings, S., Root, T. L., Seguin, B., Tryjanowski., 2007. Assessment of observed changes and responses in natural managed systems. In: Climate Change 2007: Impacts, Adaptation and Vulnerability. Contribution of Working Group II to the Fourth Assessment Report of the Intergovernmental Panel on Climate Change (ed. By M. L. Parry, O. F. Canziani, J. P. Palutikof, P. J. van der Linden & C. E. Hanson), 79-131. Cambridge University Press, UK.
84. Saavedra, F., Inouye, D. W., Price, M. V., Harte, J., 2003. Changes in flowering and abundance of Delphinium nuttallianum (Ranunculaceae) in response to a subalpine climate warming experiment. Global Change Biology. 9: 885-894.
85. Schmidt, R. H., 1979. A climatic delineation of the "Real" Chihuahuan Desert Region. Journal of Arid Environments. 2: 243- 250.
86. Schmidt, R. H., 1986. Chihuahuan climate. In Second symposium on resources of the Chihuahuan desert region. Editors Barlow, J. C., Powell, A. M., Timmermann, B. N. Alpine, Texas: Chihuahuan Desert Research Institute. 40-63.
87. Schwartz, M. D., Reiter, B. E., 2000. Changes in North American spring. International Journal of Climatology. 20: 929-932.
88. Smith, S. D., Monson, R. K., Anderson, J. E., 1997. Physiological ecology of North American desert plants. Springer-Verlag Berlin Heidelberg New York. 3-540-53113-0
89. Sparks, T. H., Menzel, A., 2002. Observed changes in seasons: an overview. International Journal of Climatology. 22: 1715-1725.

90. U.S. Department of Agriculture, Forest Service. Range plant handbook. Washington DC. 532p.
91. Vanamburg, L. K., Trlica, M. J., Hoffer, R. M., Weltz, M. A., 2006. Ground based digital imagery for grassland biomass estimation. International Journal of Remote Sensing. 27 (5-6): 939-950.
92. Van Auken, O. W., 2000. Shrub invasion of North American semiarid grasslands. Annual Review Ecology Systematics. 31: 197-215.
93. Waide, R. B., Willig, M. R., Steiner, C. F., Mittelbach, G., Gough, L., Dodson, S. I., Juday, G. P., Parmenter, R., 1999. The relationship between productivity and species richness. Annual Review Ecology Systematics. 30: 257-300.
94. Welsh, R. G., Beck, R., F., 1976. Some ecological relationships between Creosotebush and bush muhly. Journal of Range Management. 29(6): 472-475.
95. Whitford, W. G., Anderson, A., Rice, P. M., 1996. Stemflow contribution to the "fertile island" effect in Creosotebush, *Larrea tridentata*. Journal of Arid Environments. 35: 451-457.
96. White, M. A., Nemani, R. R., 2006. Real-time monitoring and short-term forecasting of land surface phenology. Remote sensing of Environment. 104: 43-49.
97. Zhang, X., Friedl, M. A., Schaaf, C. B., Strahler, A. H., 2005. Monitoring the response of vegetation phenology to precipitation in Africa by coupling MODIS and TRMM instruments. Journal of Geophysical Research. Journal of Geophysical Research (110), D12103, doi: 10.1029/2004JD005263.

7. Curriculum Vitae

Libia Gonzalez-Alonso

Originally from Chihuahua, Chihuahua, Mexico, Libia chose to pursue a degree in Ecological Engineering at La Universidad Autonoma de Chihuahua. Her effort earned her a scholarship from Gobierno del Estado de Chihuahua, and she immersed herself in the Environmental Science program at UTEP as a Masters student in 2008. Dr. Craig Tweedie gave her the opportunity to join the Systems Ecology Lab first as a research assistant, and finally becoming a full time student. She had the great opportunity to work on the establishment of a cyberinfrastructure located at Jornada Experimental Range where she was able to develop her thesis for the completion of her Masters in Science in the Environmental Science Program at the University of Texas at El Paso, 2001.

411 New York Av.

El Paso TX 79902